



Principles of Photocatalysts and Their Different Applications: A Review

Mohamed A. Hassaan¹ · Mohamed A. El-Nemr² · Marwa R. Elkatory³ · Safaa Ragab¹ · Violeta-Carolina Niculescu⁴ · Ahmed El Nemr¹ 

Received: 24 July 2023 / Accepted: 11 October 2023 / Published online: 31 October 2023

© The Author(s) 2023

Abstract

Human existence and societal growth are both dependent on the availability of clean and fresh water. Photocatalysis is a type of artificial photosynthesis that uses environmentally friendly, long-lasting materials to address energy and environmental issues. There is currently a considerable demand for low-cost, high-performance wastewater treatment equipment. By changing the structure, size, and characteristics of nanomaterials, the use of nanotechnology in the field of water filtration has evolved dramatically. Semiconductor-assisted photocatalysis has recently advanced to become among the most promising techniques in the fields of sustainable energy generation and ecological cleanup. It is environmentally beneficial, cost-effective, and strictly linked to the zero waste discharge principle used in industrial effluent treatment. Owing to the reduction or removal of created unwanted byproducts, the green synthesis of photoactive nanomaterial is more beneficial than chemical synthesis approaches. Furthermore, unlike chemical synthesis methods, the green synthesis method does not require the use of expensive, dangerous, or poisonous ingredients, making it a less costly, easy, and environmental method for photocatalyst synthesis. This work focuses on distinct greener synthesis techniques utilized for the production of new photocatalysts, including metals, metal doped-metal oxides, metal oxides, and plasmonic nanostructures, including the application of artificial intelligence and machine learning to the design and selection of an innovative photocatalyst in the context of energy and environmental challenges. A brief overview of the industrial and environmental applications of photocatalysts is also presented. Finally, an overview and recommendations for future research are given to create photocatalytic systems with greatly improved stability and efficiency.

Keywords Doped metal oxides · CO₂ reduction · Plasmonic nanostructures · Photocatalyst · H₂ production · Artificial intelligence

1 Introduction

Photocatalysts are nanoparticles (NPs) with semiconducting features such as light absorption, charge transfer, and favorable electronic structure, among others. Photoactive NPs serve as catalysts in a variety of applications, including sustainable energy production and environmental remediation [1–15]. When compared with bulk materials, photocatalysts have exceptional structures and a higher surface area to volume ratio, which boosts their actions [16, 17]. As a result, controlling the shape and size of photocatalytic materials in the nanoscale range allows for the creation and fabrication of materials appropriate for use in innovative applications. Green photoactive NPs can be made from a variety of biological sources, including plant materials and microorganisms. This synthesis approach is environmentally friendly, green, biocompatible, and cost-effective [18, 19]. Green synthesis nanophotocatalysts exhibit improved catalytic activity while reducing the usage of costly and dangerous chemicals [20, 21]. The use of diverse bacterial species for the fabrication of noble metals such as Au, Ag, Pt, Pd, and other semiconductor oxides such as TiO₂ and ZnO is also favorable for greener synthesis of NPs. Algae, bacteria, and fungi have commonly been used in microbial-mediated processes to produce very stable metal NPs. Plant extracts are becoming increasingly popular owing to their ease of production and handling, as well as their low danger. Because light is plentiful, inexpensive, clean, sustainable, and readily available, photocatalytic pollution remediation is a potential solution. Furthermore, light can trigger highly selective reactions [22–25]. Photocatalysis can easily destroy persistent organic contaminants [26]. To enable light-induced reduction–oxidation (redox) processes that oxidize many organic contaminants by producing reactive oxygen species (ROS), new, high-performance, photoactive nanomaterials are required [24, 27–29]. For humans, sunlight is a crucial source of energy. A continual flow of electromagnetic radiation waves carries solar energy to the Earth's surface (Fig. 1). Only a small fraction of the total energy emitted in the solar system is captured by the planet. Photosynthesis has been

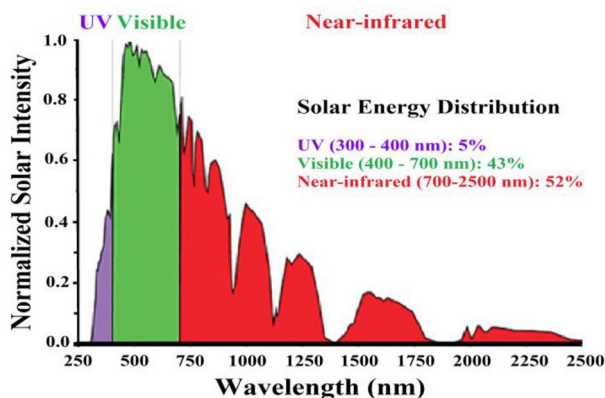


Fig. 1 The solar energy spectrum [31]

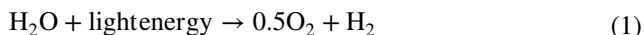
the most common method of converting solar energy into usable energy, which is vital to human survival via agriculture and forestry. Solar radiation has a total power of 384.6 yottawatts. A significant quantity of energy is radiated continuously by the Sun in all directions. Exposed parts of the Earth receive around 1368 W m^{-2} at a distance of 150 million kilometers [30, 31]. Because the atmosphere reflects 30% of the irradiated solar energy, about 1000 W m^{-2} of solar energy is received everywhere on the Earth's surface. Although the total amount of energy produced by the Sun is more than enough, the true difficulty is figuring out how to collect and use it efficiently.

The importance of the synthesis of materials from natural, renewable, and biological resources will be described below. Materials such as semiconductors, noble metals, and ceramics can be made from the above-mentioned natural resources, needing little energy and having fewer byproducts to remove [32]. Carbon-based nanostructures, for example, can be made from renewable resources including sugarcane bagasse, coconut coir, peanuts, bamboo wood, groundnut shells, and coal [33]. The calcination and filtering of the above-mentioned naturally available resources use less energy to manufacture carbon-based nanostructures. In contrast to the traditional approach for generating carbon nanostructures, advanced production techniques such as chemical vapor deposition, molecular beam epitaxy, and thermal exfoliation techniques are required. Ramirez-Rico et al. [34] and Singh et al. [35, 36] found that these processes require a lot of energy, use toxic chemicals, emit dangerous gases, and have a high production cost. More items can be made in an environmentally acceptable manner without harming our society or the environment, according to the green technology vision. The use of energy and the production of harmful emissions are both reduced when using green chemistry. Nuclear, wind, and hydroelectric energy are currently available technologies for energy distribution around the world, all being produced in a more environmentally friendly manner than through the use of fossil fuels [37, 38]. Alternative energy production systems should be introduced in a greener way to balance the total requirement for energy from the world's population. Materials are a fundamental boon to modern technology, and their performance and variety of features define the reliability and efficacy of products. Furthermore, recent progress in the development of novel materials can be used directly in energy and environmental applications. Such advanced technology can process new materials and establish a relationship between the protocol creator, material producer, designer, and developer. This is a thorough method of identifying a long-term substance for environmental activities. There will be a great global need for sophisticated materials in the energy and environmental industries in a few years. This is the only solution to avoid excessive carbon emissions and high energy consumption in energy production materials [39–41]. The current goal is to develop sustainable materials for energy and environmental-related industries; moreover, awareness of the use of sustainable materials should be promoted through education or government initiatives for the next generation. We discuss herein several greener methodologies for the fabrication of new photocatalysts. The applications of metal oxides, metal-doped metal oxides, metals, and plasmonic nanocatalysts with higher activity than bulk materials are discussed in this review. Finally, future research trends regarding photocatalytic processes are provided in detail.

2 Photosynthesis and Photocatalysts as Sustainable Energy Solutions

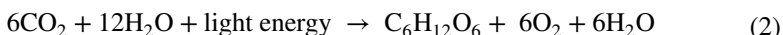
Hashimoto et al. mentioned that, in the 1970s, Fujishima and Honda introduced photocatalysis, which became known as the Honda–Fujishima effect [42–44]. Water splitting (Fig. 2) is a common type of photocatalysis, in which sunlight interacts with NP catalysts (such as TiO₂ NPs) to split H₂O molecules into O and H atoms, resulting in H₂ gas as an ecofriendly energy resource. Owing to its transparency to visible light, the efficiency of the water splitting process depends on nanocatalysts to collect light and transform it into chemical energy for water molecules.

The water splitting reaction can be described simply as



Water splitting requires light with an energy of 1.23 eV, which corresponds to a wavelength of about 1 μm [45]. In theory, every photon in the visible spectrum could cause water splitting. However, water cannot absorb sunlight directly because it is transparent to the entire spectrum.

A catalyst is required to transfer photon energy to water molecules by first absorbing the sunlight and then transferring the energy to the H₂O. Photosynthesis is the conversion of solar energy into chemical energy that can be stored in specific categories of chemical compounds. Plants break down carbon dioxide (CO₂) and water (H₂O) via photosynthesis to generate carbohydrates (C₆H₁₂O₆) and oxygen (O₂) [47–50] according to the equation



2.1 Mechanism of Photocatalytic Reactions

The activation of a photocatalyst, i.e., semiconducting material, in photocatalysis is dependent on the wavelength of the radiation and the photocatalyst's “bandgap,” that is,

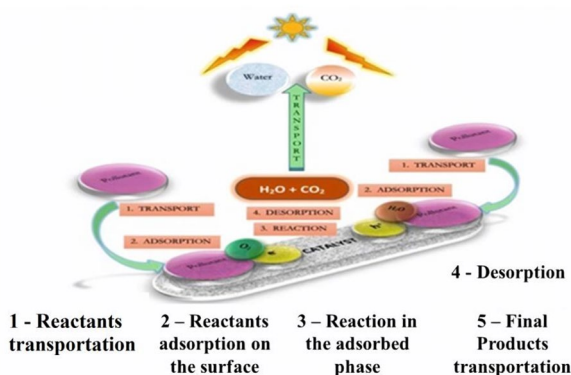


Fig. 2 The numerous processes in a heterogeneous photocatalytic reaction, modified after Ref. [46]

the energy difference between the valence band (VB) and the conduction band (CB) of the photocatalyst [51–55]. When a photocatalyst such as CdS, ZnO, WO_3 , ZnS, ZrO_2 , or TiO_2 absorbs energy from an artificial light source or sunlight, the production of an e–h pair can occur only if the photon energy ($h\nu$) is equal to or greater than the photocatalyst's bandgap energy (E_g) [55–58]. An electron in the conduction band of the semiconductor (e^- -CB) can be used to reduce any substrate, while a hole in the valence band (h^+ -VB) can be used to oxidize a variety of substances. The photocatalytic reaction can take place in two ways: homogeneously or heterogeneously [59–63], but heterogeneous photocatalysis has been extensively discussed in recent years owing to its widespread application in fields such as environmental remediation, energy-related applications, and organic syntheses [59, 63].

The following are the steps in the total photocatalysis reaction process [64], which are depicted in Fig. 3 [65, 66]:

After the incidence of a photon with energy ($h\nu$) higher than or equal to the semiconductor's bandgap energy (E_g), the photocatalytic process (step 4) commences [68]. The following are the reactions that proceed during the oxidation of organic compounds using photocatalysts under ultraviolet (UV) irradiation [69–71]:

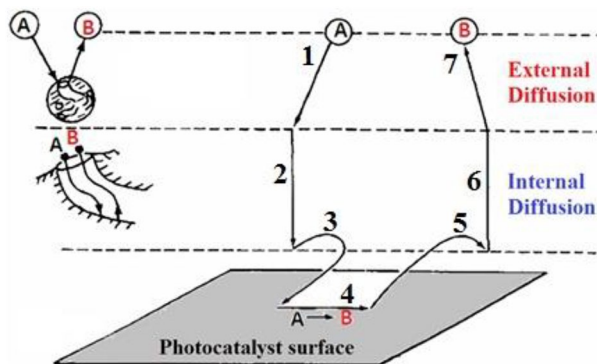
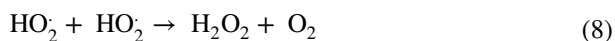
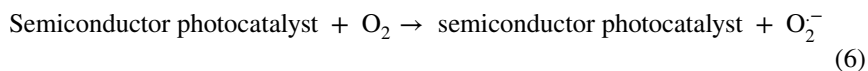
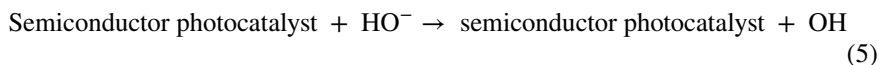
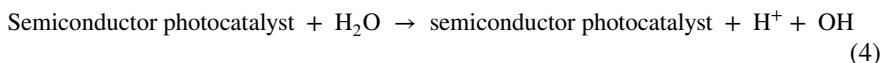
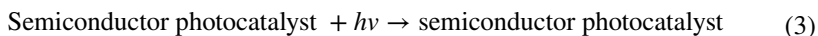
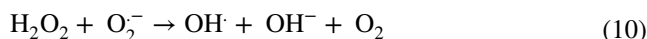
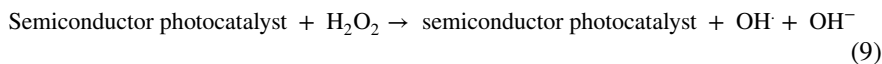


Fig. 3 Steps involved in heterogeneous catalysis, modified after Ref. [67]



When the photon energy received from the Sun or other types of artificial light sources (fluorescent lamps, light-emitting diodes (LEDs), etc.) is equal to or greater than the semiconductor photocatalyst's bandgap energy ($h\nu > E_g$), an electron in the semiconductor photocatalyst's occupied VB can be shifted to the unoccupied CB, resulting in an excited-state conduction-band electron (e^- -CB) and a positive valence-band hole (h^+ +VB) [67]. Redox processes (Eqs. 3–14) involving numerous organic compounds adsorbed on the photocatalyst surface can easily involve electron and hole migration to the photocatalyst surface. The formation of high-energy OH occurs when positively charged holes (h^+ +VB) react with surface-bound water or $\cdot\text{OH}$. While free radicals (Eqs. 3–4) react with oxygen to form superoxide anions, e^- -CB reacts with oxygen to produce superoxide anions (Eq. 6). Hydroxyl radicals are also produced by following the reaction pathway described in Eqs. 7–11. This cycle repeats until light energy becomes available. Hydroxyl radicals ($\cdot\text{OH}$) are the primary oxidizing species in photocatalytic oxidation processes [72]. In heterogeneous photocatalysis, the oxidation paths are more important than the reduction pathways [69]. The heterogeneous photocatalytic process is depicted in full in Fig. 4.

The recombination of the photoexcited e–h pair can release energy in the form of heat. As a result, e–h pair recombination is detrimental and decreases the efficacy of the operation [70]. Furthermore, the main goal of photocatalysis is to achieve

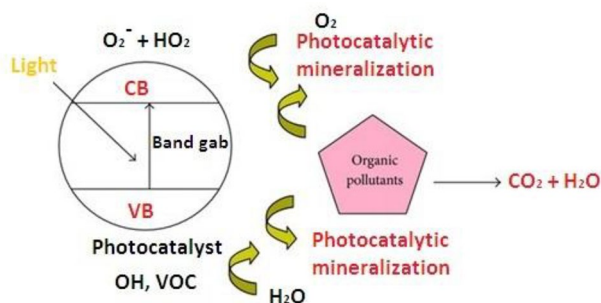


Fig. 4 Heterogeneous photocatalysis concept for degrading organic compounds in water

a high-efficiency photocatalytic interaction between the excited e^- CB and the oxidant to produce the reduced product. Furthermore, to form an oxidized component, a reaction between a positive h^+ VB and a reductant is required. After the photocatalysis reaction, CO_2 , water, and other degradation products (such as SO_4 and NO_3) are formed.

2.2 Nanostructured Photocatalysts

Numerous semiconductors have been used as photocatalysts, including metal oxides (ZrO_2 , ZnO , V_2O_5 , TiO_2 , Fe_2O_3 , WO_3 , and CeO_2) and sulfides (CdS and ZnS). TiO_2 , a semiconductor photocatalyst, has gained popularity as a result of its capacity to degrade organic contaminants found in waste streams [73–75]. In aqueous conditions, this photocatalyst shows improved conformity between photocatalytic performance and stability [76]. Scientists have recently been working on developing innovative heterogeneous photocatalysts with comparatively high photocatalytic performance for the breakdown of contaminants in the presence of sunlight or UV irradiation [28, 29, 77–80]. It is worth mentioning that the synthesis of photocatalysts is critical from both an economic and practical standpoint [64].

Nanostructured photocatalysts are extremely small semiconductor particles that are only a few nanometers in size. During the last decade, the photochemistry of nanostructured photocatalysts has become a significant domain of study in physical chemistry [81]. The improved photocatalytic and photophysical capabilities of these nanostructured photocatalysts in comparison with bulk materials piqued researchers' curiosity [82, 83]. The enhanced specific surface area and quantum size (Q-size) are primarily responsible for the aforesaid properties. The quantum size effects are caused by limited electron movement when the particle size of photocatalysts is less than a critical size limit (for example, when the particle size is reduced to the nanometer scale). Owing to the direct effect of quantum size, the semiconductor photocatalyst's CB and VB can become discretized into energy levels. This discretization process is determined by the size of the material structure. The redox potential of the VB or the CB changes more positively or negatively as a result of discretization. The redox potential of the produced electrons and holes is increased in this way. As a result, nanostructured photocatalysts become more reactive to oxidation [15, 70, 84].

Another important consideration for catalysts is the particular surface area. The availability of additional atoms on the particular surface of the semiconductors improves the adsorption ability of nanostructured photocatalysts. The time it takes for $e-h$ pairs to undergo interaction with the surface of semiconductor particles determines the photocatalytic efficiency of any photocatalyst. If the particle is in the nanoscale range, the diameter becomes insignificant, and the transfer of $e-h$ pairs from the interior to the surface turns out to be very easy, increasing the rate of the redox reaction. Because the transport of $e-h$ pairs to the surface from the interior of the catalyst is enhanced, the likelihood of $e-h$ pair combination decreases for nano-photocatalysts. As a result, enhanced photocatalytic reactions can be accomplished, so nanostructured photocatalysts exhibit higher photocatalytic activities than bulk

photocatalysts [85, 86]. A semiconductor catalyst's photocatalytic performance is greatly dependent on its porosity distribution. The most effective catalysts have an ideal porosity distribution in the range of micro- (pore sizes < 2 nm) or mesoporous (pore sizes 2–50 nm) range. Auyeung's group published a paper on a method for regulating the structure and porosity of catalytic NPs [87]. The existence of enormous mesopores and macrosized pores increases the operative transfer of reactants for modifying the diffusional constraints during photocatalytic activities in the case of enforced nanotexture heterogeneous catalysts (such as mesoporous sieves, zeolites, etc.). As a result, both the porosity distribution and pore size play a significant role in the real-world application of well-designed nanosized porous photocatalysts [88].

3 Different Approaches for Synthesis of NPs

The “top-down” technique and the “bottom-up” approach (Fig. 5) are the two basic approaches for NP synthesis. NPs are manufactured via size reduction, dissolving from bulk material into small particles, in the top-down manner [89]. Physical and chemical processes such as lithography, mechanical (e.g., milling, grinding), sputtering, chemical etching, thermal evaporation, pulsed laser ablation, and photoreduction can be used to accomplish this procedure [90–94]. The top-down technique, on the other hand, has a key flaw: the surface structure is incomplete [95]. Wet chemical methods (e.g., chemical reduction/oxidation of metal ions) and others, such as sol–gel chemistry, chemical vapor deposition (CVD), coprecipitation,

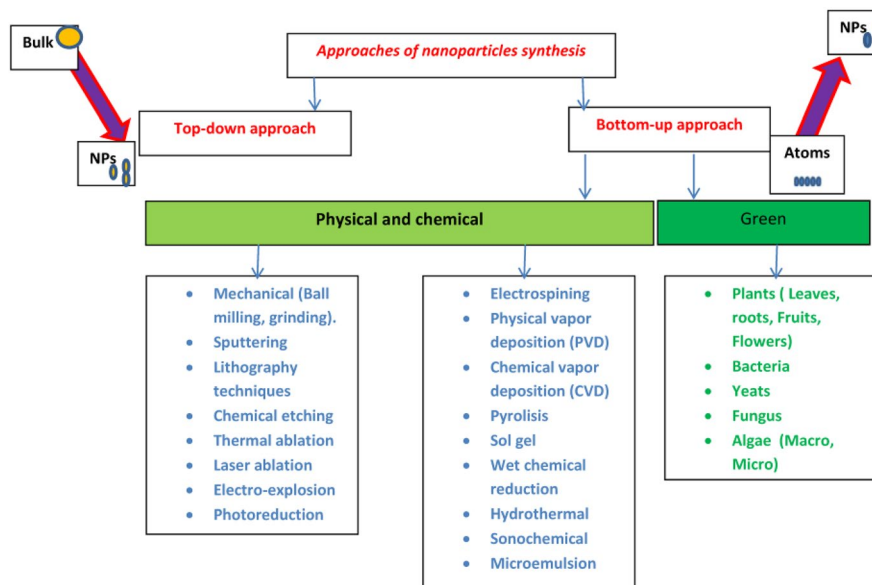


Fig. 5 Various approaches to NP synthesis

microemulsion, pyrolysis, hydrothermal, solvothermal, radiation-induced, and electrodeposition methods, are used in the bottom-up approach [96–105]. Bottom-up synthesis, also known as the self-assembly technique, involves assembling NPs from smaller units such as atoms, molecules, and smaller particles [106, 107]. They are, however, disadvantageous because of the use of potentially dangerous and poisonous ingredients, high investment costs, environmental toxicity, high energy demands, long response times, and non-ecofriendly byproducts [108–110].

As numerous terminologies and concepts converged and diverged to build a web of green chemistry, the philosophy of green synthesis took its natural course. Figure 6 depicts the web or connectivity between various green synthesis subdisciplines. The “nano” universe is too big to be categorized into a single mode. As a result, the classification of NPs is governed by several factors, including their size, shape, content, homogeneity, and aggregation [5]. Figure 7 depicts a variety of traditional methods for the classification of NPs.

4 What Is Green Synthesis?

With the publication of Rachel Carson’s *Silent Spring* in 1962, the environmental agenda gained traction, resulting in the establishment of the US Environmental Protection Agency (EPA) and the birth of green chemistry. Over time, this strategy became increasingly popular among scientists. The philosophy of green synthesis is to synthesize chemicals and molecules in an environmentally acceptable manner. NPs are no exception when it comes to using this method of synthesis.

The following are the main goals of green NPs synthesis:

- Using solvents/reagents that are safe for synthesis

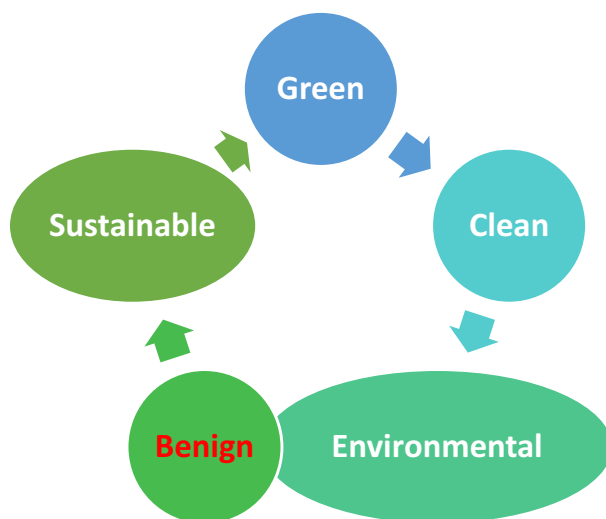


Fig. 6 Alternate nomenclatures for environmentally friendly techniques shown in the web of green chemistry

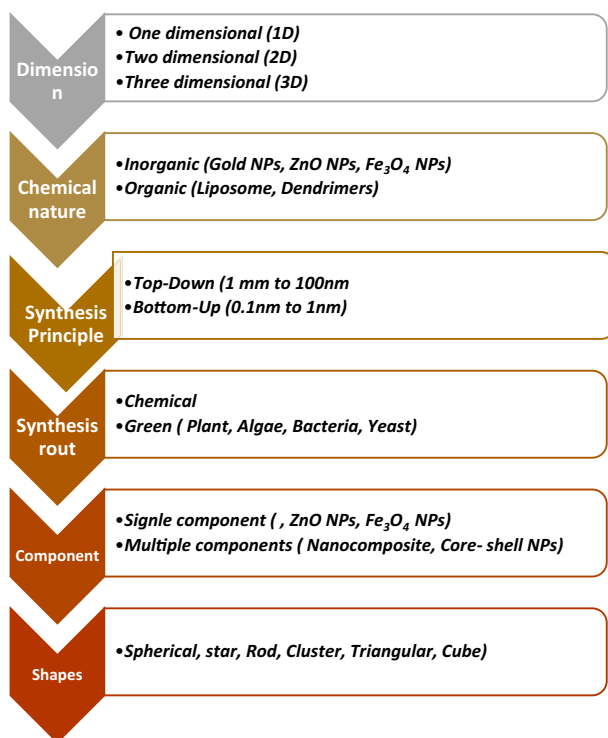


Fig. 7 The classification of NPs through various modes

- Using a low-energy conversion technique
- Using a biological process to make NPs (i.e., a biosynthetic route)
- Achieving environmentally friendly and safe NP synthesis for future applications

4.1 How Is Synthesis Green?

As previously stated in the principles of NP synthesis via green chemistry, the main emphasis is on the environmentally friendly characteristics of the process and final product to avoid any form of hazard. Table 1 outlines a small number of attempts at manufacturing NPs that are environmentally friendly.

4.2 What Are the Approaches for Green Synthesis of NPs?

NPs can be made using a variety of techniques. However, the process can be changed with good reason to fulfill the goal of green synthesis. Table 2 summarizes a few of the green synthesis pathways.

Table 1 The logic for using a green approach for synthesis of NPs

No.	NPs	Mode of synthesis	Why green?	Refs.
1	Co	Reduction of <i>p</i> -nitrophenol to <i>p</i> -aminophenol by sodium borohydride	The manufacture of air-stable NPs is made possible by a simple reduction method	[111]
2	Magnetic NPs based on Fe ₃ O ₄	One-pot solvothermal method	Synthesis time is reduced by 30 min	[112]
3	Ag	Cow milk as reductant	Cow milk proteins reduce Ag ⁺ ions, making it an excellent phytopathogen inhibitor	[113]
4	Ag and Au	Calcium alginate gel beads using a reductant and a stabilizer	For solid-phase biopolymer-based catalysts, a green photochemical method has been proven to be helpful	[114]
5	Au	Amine as a reducing agent and stabilizer	Using amine-reducing agents, we were able to control the creation of Au NP structures	[115]

Table 2 Various green synthesis methods [5]

Type	Description
<i>Plant</i>	A common approach to green nanotechnology is to use phytochemicals, carbohydrates, and biomolecules from plant extracts (Fig. 8), as reducing or capping agents for NP formation. Among all common bioreductants, plant extracts are more beneficial than other biological resources (Fig. 9). Plant-based NP production is a simple procedure that includes mixing a metal salt with a plant extract and allowing the reaction to complete at room temperature in minutes to a few hours. Properly sized NPs are created from a metallic salt solution [116]. Plant extracts can also be used to control particle size growth by modifying synthesis parameters such as the reducing agent concentration, pH, temperature, or ratio of the reactant mix
<i>Microbes</i>	Because of their genetic diversity, widespread presence, ease of access, ease of cultivation and maintenance, ease of screening, and potential for changing the structural and functional properties of NPs, microbes have proven to be an ideal choice. The technique has grown more selective and suitable as microorganisms have a variety of biocatalysts
<i>Solar energy</i>	Sunlight, the most plentiful renewable energy source on the planet, can also be utilized to mediate the synthesis of NPs, a nonbiological route to green synthesis in general. Sunlight is a great contender for green synthesis owing to its availability and environmentally benign nature
<i>Microwave (MW)</i>	Alternative energy sources are paving the way for “green chemistry,” which can significantly reduce reaction temperatures and times while reducing energy consumption. MWs are a type of electromagnetic wave consisting of pure energy radiated as a wave traveling at the speed of light. The propagation of microwaves in condensed matter is slower than in air or vacuum, where the speed of light is slower. The power and time required for production of NPs using microwaves must be regulated. Hydrothermal synthesis devices can also benefit from microwaves
<i>Ultrasound (US)</i>	Ultrasound is a nonbiological way of producing green NPs that is safe and clean. The fabrication of controllable NPs is possible. US, which has frequencies as high as 20,000 Hz, is a powerful energy carrier that allows bulk precursors to be easily broken down into NPs of a precise shape for specific applications [117]
<i>Mild reducing agents</i>	The concentration of reducing agents and stabilizing precursors has a significant impact on metal NP synthesis. This method of NP production is essentially a hydrothermal or solvothermal process. The reactant ions and/or molecules react in a compressed liquid environment, where the reactants' dispersion is significantly superior. The presence of functional groups in the reducing or stabilizing agents has a significant impact on the NP morphology. When glucose and fructose are utilized as reducing agents, for example, changes in morphology and dispersity might be detected [118]. The reason for this is due to changes in the reaction processes of the active functional groups, which result in metal ion reduction for NP production
<i>Mild reaction conditions</i>	The synthesis process is made less dangerous and ecologically friendly by using mild reducing conditions such as ambient temperature, pH, solvent concentration, and mild surfactants as reducing agents and stabilizers. This also reduces the amount of energy required, making synthesis safer and easier

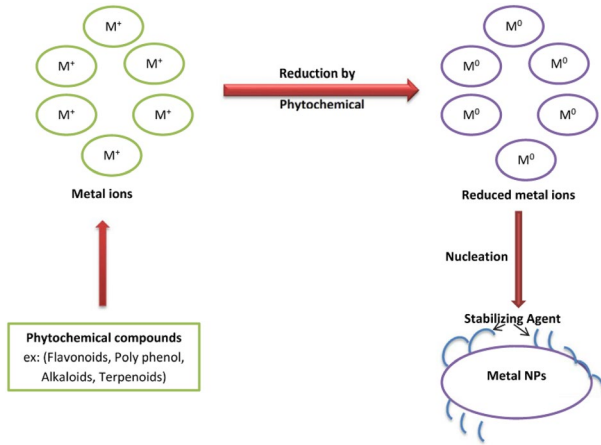


Fig. 8 The mechanism of NP fabrication by plant leaf extract, modified after Refs. [5, 119]



Fig. 9 Benefits of plant-extract-mediated NP synthesis

4.3 Green Synthesis of Different NPs and Their Applications

Figure 8 depicts several bioactive molecule compounds that have been applied in the bioreduction of metal NPs utilizing plant extracts, as well as the general bioreduction mechanisms enabled by diverse biomolecular compounds.

Alkaloids, flavonoids, saponins, steroids, terpenoids, tannins, proteins, vitamins, reducing sugars, nitrogenous bases, amino acids, and other natural phytochemical substances all contribute to metal ion reduction in plants [5, 120]. These bioactive compounds are thought to induce bioreduction in the following way:

The metal ions go through an activation phase during which they are reduced from their salt counterparts by the action of plant biomolecule metabolites with reduction capabilities, resulting in a slow development rate of particles. In the nucleation phase, new NPs are produced, and reduction processes take place as biometabolite-reducing agents, such as flavonoids or terpenoids, engage with metal ions via ionic bonding [121]. The presence of electrons as well as carbonyl groups in their molecular structure is thought to be responsible for the adsorption of biomolecule metabolite reductants on the surface of metal NPs. This is followed by a growth phase, during which the separated metal ions unite to produce metal NPs while metal ions are progressively reduced. During this process, metal ions are transformed from monovalent to divalent oxidation states to zero-valent states.

NPs merge to produce a variety of morphologies as they expand, including spheres, triangles, hexagons, pentagons, rods, wires, and cubes [122]. The longer nucleation stage may result in aggregation of the resulting NPs, altering their morphologies, whereas the continuous growth stage leads to increased thermodynamic stability of NPs. Plant metabolites crown the final step of the termination phase, in which the NPs achieve their most actively helpful and stable form [123, 124]. This mechanism, together with the synergistic adsorption of functional groups from plant extract components, will create steric repulsion, limiting NP aggregation. Figure 10 shows a more detailed depiction of this potential procedure.

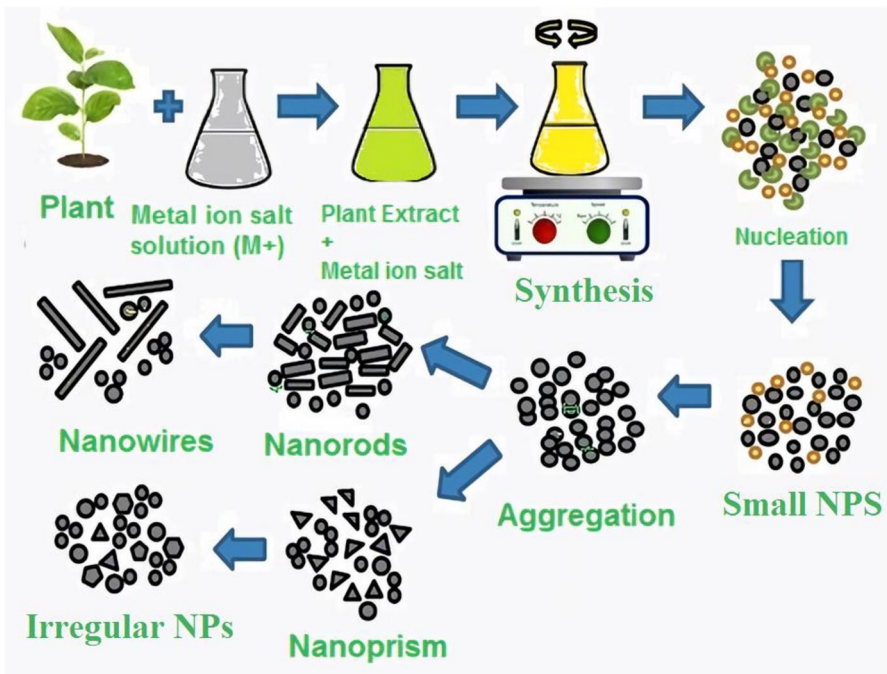


Fig. 10 Proposed green synthesis mechanism of metal NP formation, modified after Ref. [5, 125]

4.4 Green Photocatalysis

Fujishima and Honda described the process of splitting water into hydrogen and oxygen with the use of metal oxide photocatalysts under UV light for the first time in 1972. This work has since been expanded beneficially, yielding major efficiency gains [126]. Owing to the significant potential in the realm of energy and environmental challenges, this field has piqued the interest of academics since 1972. Metal oxide semiconductors have played an important role in photocatalysis for decades owing to their high reactivity, stability, chemical inertness, and low cost. TiO_2 , ZnO , MoO_3 , Fe_3O_4 , and other metal oxide semiconductors are ideal materials for water remediation, hydrogen fuel production, removal of toxic waste from water bodies, and pharmaceutical waste removal applications [56, 127–129]. These materials have outstanding physicochemical, electronic, and structural properties that enhance their performance in the applications stated. The process of transforming solar or light energy into chemical energy is known as photocatalysis. The terms “photo” and “catalysis” both refer to the process of speeding up, breaking down, or degrading a chemical reaction. Overall, photocatalysis helps to degrade harmful contaminants in aqueous solution by breaking them down with the use of light energy and successfully activating chemical reactions [130].

Photocatalysts can be divided into various categories, with modern research focusing on three of them: semiconductor photocatalysts, plasmonic photocatalysts, and heterogeneous photocatalysts. The following sections go over the results of a detailed survey of each kind. In general, green photocatalysis is a synthetic approach that aids in the preparation of various photocatalysts using natural resources, biomasses, and biological extracts [131]. Those precursors (resource materials) are environmentally friendly, green sources, offering economically viable routes for converting light energy to chemical energy over semiconducting materials, such as removing pollutants from water bodies, reducing toxic molecules, and producing hydrogen fuel [131–133].

4.4.1 Sunlight-Driven Photocatalysts

One of the most significant problems in the discipline of materials science is identifying acceptable metal oxide semiconductors for use as photocatalysts for the treatment of pollutants in water systems utilizing solar energy. A perfect photocatalytic material would have the required bandgap qualities to absorb a broad range of the solar spectrum, dissociate water molecules, and remain stable in a water environment during reaction processes. It should also be cost-effective, simple to process, readily available, and nontoxic to the environment. Various metal oxide semiconducting-based nano-assemblies have been created and proven to act as catalytic materials for water remediation under sunlight throughout the past few decades. The transition or d-block metal ions have shown excellent efficiency in semiconductors that have been extensively investigated as effective photocatalytic materials [28, 29].

The following factors affect the photocatalyst process:

(a) **Dye concentration:** A significant aspect of the photocatalytic reaction is the dye concentration. The catalyst should be capable of degrading a reasonable

amount of dye. A small amount of dye is adsorbed on the catalyst's surface, which causes a photocatalytic reaction in light-stimulated conditions. The adsorption of dye on the photocatalyst surface is proportional to the dye concentration at the start. The initial dye concentration is an important parameter that should be closely checked. The proportion of dye degradation reduces with increasing dye concentration, but the needed quantity of photocatalyst must be conserved [134].

(b) **Catalyst amount:** The amount of catalyst used in the photocatalytic reaction has an impact on dye degradation. In a heterogeneous photocatalytic process, one can increase the amount of photocatalyst in the reaction process to raise the proportion of dye photodegradation. More active sites are created in the photocatalytic reaction by increasing the catalyst number, which results in more reactive radicals being formed during photodegradation [135].

(c) **pH:** The pH of the solution is also important in the degradation process. Depending on the nature of the material and the qualities of the pollutant, the photocatalytic reaction can be either induced or suppressed by it. The surface potential of the catalyst (metal oxide NPs) can be altered by changing the pH of the solution. Pollutant adsorption on the photocatalyst surface may be affected as a result, causing an alteration in the photodegradation rate [136].

(d) **Surface morphology of the photocatalyst:** Significant parameters to be examined for photodegradation activity, such as particle size and shape, are included in the surface morphology. Each morphology is the result of a direct interaction between the catalyst's surface and the organic contaminant [137]. The quantity of photons striking the photocatalyst's surface can regulate the rate of photocatalytic activity. If the photocatalyst exhibits a range of morphologies, the reaction proceeds more quickly [138].

(e) **Surface area:** Materials with larger surface area should be used to achieve higher photocatalytic performance. Many active sites can be generated on the photocatalyst surface using these materials, resulting in the production of more radical reactive species for effective photodegradation [139].

(f) **Temperature-dependent reaction:** The temperature of the reaction should fall within this range of 0–80 °C to achieve efficient photocatalytic activity. When the temperature rises over 80 °C, the catalyst promotes e–h pair recombination and suppresses photocatalytic activity. As a result, the reaction temperature is critical for the photocatalytic activity [140, 141].

(g) **Nature of the pollutants and their concentrations:** The number and composition of specific contaminants in a water matrix can impact the degree of photodegradation. When the pollutant concentration is higher, toxic pollutants cannot be addressed by photocatalysts such as TiO₂ as this saturates the photocatalyst surface and prevents the formation of active radicals, lowering the photocatalytic effectiveness [142].

(h) **Irradiation period and intensity of the light:** The incoming light intensity and irradiation period are important parameters in pollutant photodegradation. The photodegradation percentage is inversely related to the intensity of light at high light intensities owing to the production of excitons and the sluggish recombination of e–h pairs. Alternatively, the photocatalytic surfaces undergo

e–h pair recombination, which decreases the reaction medium’s catalytic activity when the light intensity is increased [143].

i. **Dopants on dye degradation:** TiO₂ NPs that absorb photons at very low energies can be made using a variety of ways. Bandgap engineering entails the insertion of metals and nonmetals into photocatalytic materials to continuously alter and move the VB and CB. Surface modification can be accomplished by combining organic and semiconductor materials [144].

4.4.2 Metal Oxides

Photocatalysis using semiconducting metal oxide-based nanostructures has been applied to clean wastewater and manufacture hydrogen fuel by splitting oxygen and hydrogen, among other things. The most important qualities of a photocatalytic material are its bandgap, optimum band-edge position, large surface area, perfect morphology, chemical stability, and reusability. TiO₂, ZnO, SnO₂, Cu₂O, and WO₃ with these parameters have identical photocatalytic properties, such as light absorption, among diverse metal oxide semiconductors. This stimulates photogenerated charge carriers, resulting in the formation of holes that are capable of oxidizing organic compounds [145]. Direct sunlight, visible light, ultraviolet (UV) light, or a combination of both are used to activate semiconducting metal oxide nanostructures in this reaction. The e–h pairs are formed when photons excite charge carriers from the VB to the CB. The oxidation and reduction reactions that break down the molecular chains of organic contaminants use these photogenerated e–h pairs. The semiconducting metal oxide’s photocatalytic activity is based on two broad features [146]: (i) the oxidation of OH[−] anions to produce hydroxyl radicals, and (ii) the reduction of O₂ to produce superoxide radicals. These radical reactive species can disinfect or mineralize organic contaminants into harmless byproducts. As a result, this process has enormous scientific significance in the fields of the environment, hydrogen fuel production, and energy. Photocatalytic materials are commonly used to remediate wastewater by removing pathogens and other hazardous contaminants.

The bandgaps and band-edge positions of various commonly used photocatalytic semiconducting materials are shown in Fig. 11 [147]. Although some of these semiconducting materials, such as ferric oxide (Fe₂O₃), have sufficient bandgap energies to act in the visible light area, their use as efficient photocatalysts suffers from certain disadvantages. Researchers are looking for alternative materials to solve these problems. Metal chalcogenide semiconductors (e.g., PbS and CdS) have been shown to exhibit photocatalytic activity. However, these show limited stability and hazardous effects, and are prone to photocorrosion. Meanwhile, metal oxide semiconductors with edges of the CB that fall below the normal hydrogen electrode (NHE) potential, such as SnO₂, WO₃, and Fe₂O₃ exhibit excellent stability and photocorrosive characteristics in aqueous solution. The charge transfer property for hydrogen evolution during water splitting is initiated by using an external voltage, according to Gupta et al. [148]. When compared with TiO₂ and ZnO materials, Fox et al. found that Fe₂O₃ showed poorer photoactivity owing to corrosion or the creation of short-lived charge transfer states between metal and ligand [131]. Bahnemann et al. [149] fabricated a ZnO material and discovered that it dissolves in water over time

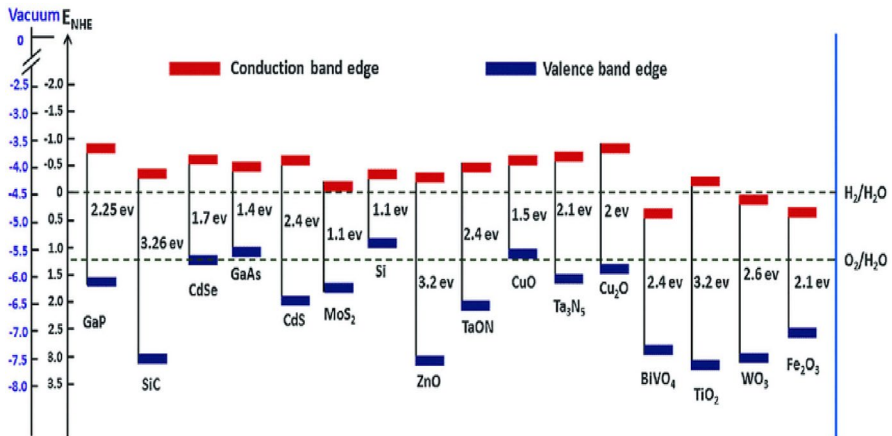


Fig. 11 Band-edge position of different metal oxide semiconductors in comparison with a standard hydrogen electrode [150]

because of its deteriorating stability. TiO₂ nanomaterial, on the other hand, is corrosion resistant and shows excellent aqueous stability.

4.4.3 Metal-Doped Metal Oxides

Doping is the introduction of impurity atoms into any semiconducting material's lattice system, as stated by Neamen [151]. The properties of the host material are influenced and engineered by the dopant atoms in the semiconductor lattices. A graphical example of faults in a lattice structure is shown in Fig. 12. Replacement or substitutional doping refers to substituting any impurity or foreign atom for one or more host atom. The following conditions must be met: (i) the crystal structure, electronegativity, and solubility states of both the host metal and the dopant metal must be the same, and (ii) the difference in atomic radii of the dopant atoms must not exceed 15%.

This type of doping is known as interstitial doping because the foreign atoms are wedged between typical lattice positions. The atoms are pushed out of the lattice, leaving voids between the host atoms. The interstitial and host atom radii can be evaluated to determine the chances of atoms entering interstitial locations. The atomic radius variations determine the precise location of the dopant atoms in the interstitial sites. Such cation/anion ratio (r^+/r^-) ionic radius measurements can be used to determine which cations will be present in certain interstitial locations. Cation coordination numbers at interstitial sites are determined by the ionic radius ratio, such as 6 (octahedral), 4 (tetrahedral), and so on. When the ionic radius ratio is increased, the number of anions surrounding the cations increases as well. Cations are wedged between anion planes in the tetrahedral holes of the tightly packed structures when the ionic radius ratio is between 0.225 and 0.414. If it lies between 0.414 and 0.732, they are filled with octahedral holes [151]. Metal or nonmetal doping or the doping of molecules with semiconductors

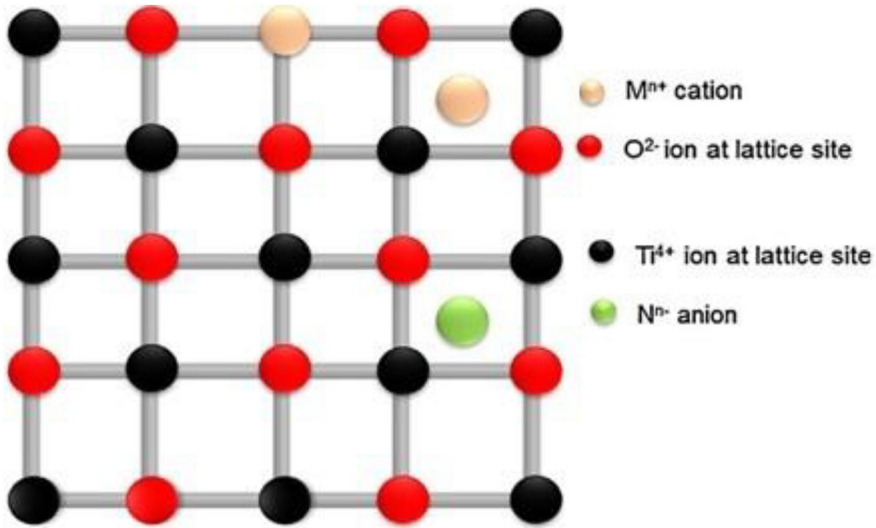


Fig. 12 Two types of doping depicted in the lattice structure of TiO_2 crystals: substitutional and interstitial doping, modified after Ref. [147]

appropriate for photocatalysis is the best strategy for increasing a photocatalyst’s absorption capabilities and modifying its electrical properties (Fig. 13). All of these factors, as well as the dopant’s surface chemical composition and ionic radius, can influence the efficacy of the doping process. Metal and nonmetal doping have received a lot of attention in recent years. Many studies have examined the use of nonmetals (e.g., boron, sulfur, and carbon) as dopants in semiconductors to change the bandgap and band-edge position of a semiconductor to make it a visible-light active photocatalyst.

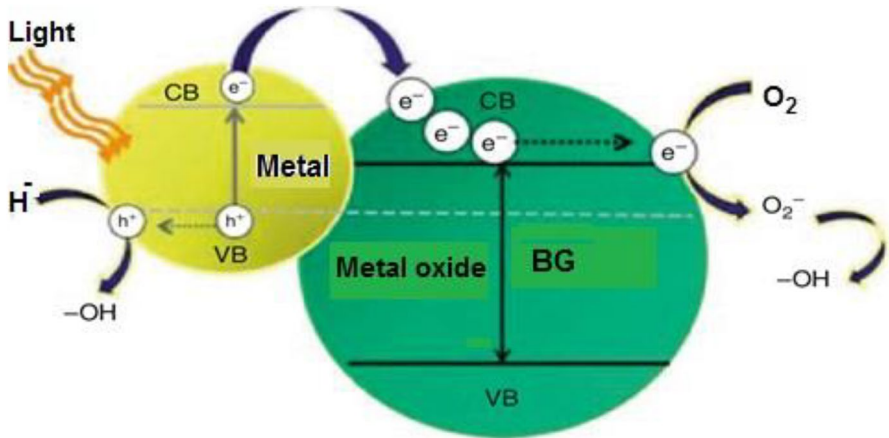


Fig. 13 A semiconducting photocatalyst doped with metal NPs, modified after Ref. [153]

Because of their greater bandgap energy, photocatalysts with semiconducting surfaces, such as TiO_2 , SnO_2 , and ZnO , can be made to operate in the ultraviolet range. It helps to change the semiconductor's electrical structure and adjust the band-edge positions by moving the absorption range of the semiconductors into the visible light area by doping with suitable metal or nonmetal ions. Under visible light irradiation, the doped semiconductor demonstrates exceptional photocatalytic performance [152]. Recent decades have seen much research into the active photodegradation of hazardous organic pollutants, pharmaceutical waste, and deadly colors by using metal-doped TiO_2 NPs under visible light. The absorption of TiO_2 in the visible spectrum may be affected by structural variations. Furthermore, since the early 1990s, extensive research has been done on TiO_2 NPs doped with nonmetals such as nitrogen, carbon, fluorine, and sulfur. These photocatalysts have demonstrated exceptional activity against a variety of contaminants when exposed to sunlight.

4.4.4 Plasmonic Photocatalysts

Plasmonic photocatalysts have piqued researchers' interest because of their improved performance under visible light irradiation, wide spectrum of sunlight absorption, and better charge transport abilities [26, 154–157]. This type of material architecture can be formed by scattering noble-metal NPs on top of a semiconductor. Two separate characteristics are achieved in this manner: localized surface plasmon resonance (LSPR) and a Schottky barrier [26, 158]. Under visible light irradiation, these characteristics will aid in the efficient separation and transfer of charge carriers in the presence of visible light. The LSPR, which denotes significant oscillation on the surface of metal NPs and semiconductor photocatalysts, is the most important property for plasmonic photocatalysis.

Because of its short diffusion length and the interfacial charge transfer effect at the heterojunction, the metal–semiconductor junction in plasmonic photocatalysts aids in efficient e–h separation and allows charge carriers to be transferred quickly. Metal NPs such as Ag, Au, and Pt exhibit resonance oscillations at specific wavelengths that depend on the NP morphology, shape, and size. Plasmonic metal NPs exhibit resonance oscillations, which can change the absorption range of a UV light-active photocatalyst (such as TiO_2) into the visible range. The surface plasmon resonance phenomenon in metal NPs can dramatically boost the visible-light absorption capabilities of a low-bandgap semiconducting photocatalyst such as Fe_2O_3 . In a very thin layer of metal NPs, the total incoming light absorption can significantly improve the electron transport capabilities of a semiconductor with weak electron transport qualities. The distance between the photogenerated e–h and the noble-metal NP surface is tiny, as is the diffusion length. The charge carriers' transport characteristics are thus improved when photons are excited [26, 159]. The most significant mechanisms involved in plasmonic photocatalysis are depicted in Fig. 14. Au NPs are partially ringed on the TiO_2 photocatalyst surface. Because of the material's excess electrons and defects in the native oxygen, TiO_2 NPs have *n*-type properties in general [160]. Conventional TiO_2 photocatalysts have been compared and analyzed thoroughly to assess the photocatalytic efficacy of Au– TiO_2 nanostructures. Figure 14 shows how NPs of Au on the TiO_2 surface can absorb all wavelengths of

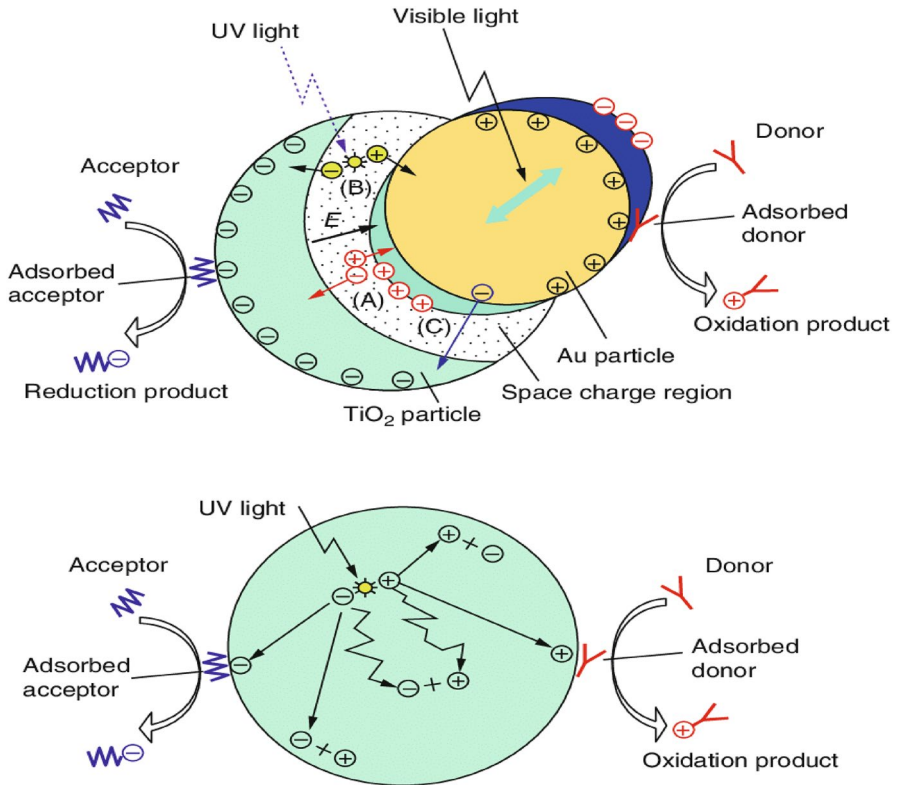


Fig. 14 Comparison of plasmonic photocatalysts with semiconductor photocatalysts, illustrating the charge transfer mechanism [26]

electromagnetic radiation in the visible spectrum, according to LSPR. TiO₂ e–h collective oscillation uses an interfacial charge transfer technique to aid in the reduction and oxidation of hazardous contaminants in an aqueous medium.

When compared with typical TiO₂ photocatalysts, this interfacial charge transfer action significantly reduces electron and hole recombination. The recombination of electron–hole pairs is a significant factor that can alter the semiconductor’s photocatalytic efficacy. One of Au’s most important functions in plasmonic photocatalysts is to make it easier to absorb visible light and to prevent electron–hole pair recombination. As a result, the material may be capable of higher photocatalytic efficiency than traditional TiO₂ photocatalysts.

4.4.5 Carbon Family

Carbon nanomaterials have recently received a lot of attention owing to their unique physicochemical, structural, optical, and electrical capabilities [161]. A wide range of nanocomposites can be created for use as conventional and traditional photocatalytic materials for light-derived water remediation applications

while retaining the advantageous properties of carbon materials [162]. Water disinfection, oil adsorption, and pathogen removal from water bodies have all been investigated using nanomaterials in various forms. The physicochemical features of carbon-based nanostructures, for example, can remove organic, inorganic, and other heavy metal contaminants from water sources. Carbon-based adsorbents are commercially available. Because of their quick photodegradation and charge transport capabilities, fullerenes, graphene, and carbon nanotubes are currently utilized as cocatalysts for traditional photocatalytic materials such as TiO_2 , ZnO , SnO_2 , and others. Above all, carbon-based nanomaterials have the potential to break down complex and dangerous contaminants in water bodies with high efficiency. Under UV light illumination, graphene-decorated TiO_2 nanocomposites have demonstrated high photocatalytic activity, according to Kamat et al. [163]. This nanocomposite breakthrough was demonstrated in depth using numerous material combinations for improved activity. As a result of their excellent physicochemical properties, strong electron-accepting capacity, regulation of work function, and electronic characteristics, graphene and its derivatives outperform other carbon nanostructures in catalysts against a variety of contaminants. These characteristics make graphene-based nanocomposites great candidates for photocatalytic applications, as they can modify the photocatalytic performance of semiconductors. Suárez-Iglesias et al. used a variety of photocatalysts to generate variations in morphology, joining with graphene via electrostatic interaction or chemical bonding for photocatalytic applications. Organic, inorganic, a combination of metalorganic frameworks, semiconductors, plasmonic metals, nonmetal plasmonic materials, and dyes are all employed as photocatalysts [164].

Catalytic materials such as graphite, activated carbon, and soot have long been replaced by carbon nanotubes (CNTs) because of their superior catalytic properties [162, 165]. Because CNTs have many active sites and a large surface area, they have recently been discovered to be effective at absorbing some hazardous chemicals. When compared with pristine CNTs and pristine TiO_2 , the integration of TiO_2 into the CNT matrix has proved to result in an effective photocatalytic material with increased activity. The valence band traps electrons, allowing a broad range of visible light to be absorbed. The recombination rate of e–h pairs may be greatly reduced by using these nanocomposites. The energy gap of the composite nanostructures can be reduced to achieve visible light absorption of the nanocomposite.

Organic materials provide additional energy and environmental advantages, such as chemical inertness, affordability, and the capability to tackle a wide range of environmental challenges. Metal–organic frameworks, graphitic carbon nitride, and various organic dyes can be linked together with graphene or CNT nanostructures, metal–organic frameworks, graphitic carbon nitride, and other organic dyes to be employed as photocatalysts [166]. During the coupling, a Schottky-type heterojunction is formed between the organic semiconductor and graphene surfaces, which efficiently facilitates charge transport throughout the junction. The structural, electrical, and physicochemical features of graphene–organic semiconductors are facilitated by this type of layered design with metal-free photocatalysts, resulting in remarkable photocatalytic performance. Using graphene/g- C_3N_4 nanocomposites, Xiang et al. demonstrated the use of a combination of chemical

reduction and impregnation techniques. The authors claimed that, by splitting water into hydrogen and oxygen, this material might generate hydrogen.

4.4.6 Z-Scheme in Photocatalysis

Because they are capable of capturing the visible spectrum of electromagnetic radiation and causing multiple photodegradation reactions, the design and development of properly assembled metal oxide-based semiconducting photocatalysts are encouraging the use of nanomaterials to address environmental issues. In photocatalysis, the development of the Z-scheme has many advantages, including excellent sunlight harvesting capability, a high degree of redox competency, as well as the ability to quickly create active species for oxidation and reduction processes, all of which contribute to improved photocatalytic activity (Fig. 15). In such a photocatalysis system, two semiconducting photocatalyst materials are connected by an appropriate redox mediator in the Z-scheme. This technology is more efficient at utilizing or absorbing sunlight than a traditional photocatalysis system. In addition, the quantity of energy required to activate the Z-scheme is reduced. Any of the photocatalysts in this system can be used as a water oxidation and reduction potential dual-purpose system. Tada et al. described a method for making CdS–Au–TiO₂ nanocomposites and how charge transfer processes affect the photocatalytic activity. In more detail, Au NPs can be placed between CdS and TiO₂ NPs, influencing the TiO₂ photoinduced electron transfer and CdS NPs photoinduced hole transfer. Thereby, the photoinduced electrons have a strong reduction ability on CdS, while photoexcited holes have a significant oxidation ability on TiO₂ NPs. A shuttle redox mediator system is another name for this electron transport mechanism. Only Z-scheme photocatalysts benefit from this type of charge transfer mechanism. These two semiconducting systems are known as Z-scheme photocatalysts because the charge transfer processes in them resemble the shape of the letter “Z” [63, 167–170].

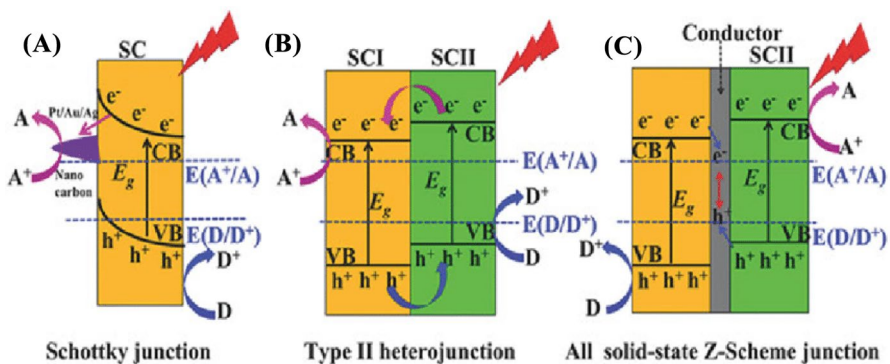


Fig. 15 Three alternative kinds of photocatalysis system, illustrated with a band-edge diagram [166]

5 Green Materials for Green Photocatalysts

5.1 Green Synthesis of Novel Photocatalysts by Microorganisms (Bacteria, Fungi, and Algae Biosynthesis) (Table 3)

The employment of microbial organisms (bacteria, fungi, yeasts, actinomycetes, viruses, etc.) in nanotechnology and microbial biotechnology is linked to the creation of innovative photocatalysts in a more environmentally friendly manner [171]. Photocatalytic NPs have been widely synthesized using prokaryotic bacterial species. Bacterial synthesis is a suitable alternative for NP manufacturing because of their easy availability in the environment and capacity to adapt to harsh environmental conditions. Bacteria are normally easy to grow and cultivate, and their biosystem may be altered easily [96, 172]. Khan and Fulekar, for example, created NPs of TiO_2 in the size range of 15.23–87.6 nm by using *Bacillus amyloliquefaciens* bacterial culture. The bacterial species were collected and isolated from effluents of the dairy sector in Mehsana, India. It is worth noting that Fourier-transform infrared (FTIR) spectroscopy revealed the presence of α -amylase, which is primarily involved in the manufacture of TiO_2 NPs (NPs). Under artificial UV exposure, NPs of biosynthesized TiO_2 showed photocatalytic degradation of the dye Reactive Red 31 (RR31) [173]. Dhandapani et al. [174] used *Bacillus subtilis* (FJ460362) bacterium to make TiO_2 NPs with a diameter of 10–30 nm. The formation of an aquatic biofilm was used to test the photocatalytic activity of the produced TiO_2 NPs. They also discovered that photocatalysis produced H_2O_2 , which inhibited biofilm formation. *Bacillus licheniformis* microbial strains (MTCC 9555) were used to produce ZnO nanoflowers (200 nm to 1 μm in diameter). Methylene Blue (MB) was used as a model pollutant to test the photodegradation efficiency of the ZnO nanoflowers. Within 60 min, ZnO nanoflowers showed 83% decolorization efficiency. After three recycles, ZnO nanoflowers showed good photostability, according to the authors [175]. Fungi, unlike other microbes, may easily create NPs owing to the presence of enzymes, proteins, and reducing agents on their cell walls. Metal salt solution is quickly reduced in the presence of enzymes on the cell wall, resulting in extracellular NPs. Because of the large-scale production and the ease of processing downstream, this is a financially feasible method. Jain and colleagues demonstrated the production of zinc oxide NPs from zinc salt using *Aspergillus* sp. NJP02, a fungal species. Zinc oxide NPs were produced extracellularly by *Aspergillus* sp. from zinc acetate. UV-induced degradation of the dye Methylene Blue (MB) was demonstrated. The photocatalytic degradation performance of zinc oxide NPs has been reported [176]. The fungus *Trichoderma harzianum* was also utilized to make cadmium sulfide NPs (CdS NPs) in the size range of 3–8 nm with a UV absorption peak at 332 nm. Photocatalytic decomposition of Methylene Blue (MB) dye in a reactor was utilized to test the photocatalytic degradation performance of the biologically generated CdS NPs. After 60 min, with a reaction rate of 0.0076 min^{-1} , the degrading efficiency was reported to be 37.15% [177]. Algae are basic photosynthetic, autotrophic organisms that may be unicellular (e.g., *Chlorella*) or

Table 3 Different biobased sources for photocatalyst nanoparticle synthesis and their different applications

Extract type	Photocatalyst	Size	Shape or application	Refs.
<i>Fusarium oxysporum</i>	ZnS	42	Spherical	[200]
<i>Fusarium oxysporum</i>	CdS	5–20		[201]
<i>Cortolus versicolor</i>	CdS	8–15	Globular	[202]
<i>Phanerochaete chrysosporium</i>	CdS	1.5–2	Spherical	[203]
<i>Calotropis gigantean</i>	CdS	20	86% MB and 91% EY removal	[204]
<i>Citrus limetta</i>	ZnS	27	83% RhB removal	[205]
<i>Corymbia citriodora</i>	ZnS	45	96% MB removal	[206]
<i>Ficus johannis</i>	ZnS	1.4	> 90% Naph, AnT, 4-CP, 4- <i>i</i> -NP removal	[207]
<i>Dicliptera roxburghiana</i>	CdS	2.5–8	87% MB removal	[208]
<i>C. maxima</i> peel	Iron nZV	10–100	-	[209]
Green tea extracts	Iron NPs		photoactive	[210]
Pomegranate (<i>P. granatum</i>)	Iron NPs		Photocatalyst	[211]
<i>Tamarix aphylla</i>	Iron NPs		Spherical iron oxide nanoparticle	[211]
<i>Cynometra raniflora</i>	Iron NPs		Photocatalyst	[212]
<i>K. alvarezii</i> plant extract	Iron NPs		Dye degradation	[213]
<i>Peumus boldus</i>	Silver NPs		18 nm spherical	[214]
<i>Terminalia catappa</i> leaf extract	Copper Nps		Tensile strength and thermal stability	[215]
<i>A. sativum</i> , <i>A. cepa</i> , and <i>P. crispum</i>	ZnO NPs		Photoactive	[216]
<i>Daphne mezereum</i>	Iron oxide NPs		Photocatalyst	[217]
<i>A. indica</i>	Iron oxide NPs		Antibacterial and photocatalyst	[218]
<i>Cynometra raniflora</i>	Iron oxide NPs		Photocatalyst	[219]
<i>Rhodobacter sphaeroides</i>	ZnS	6.8	Spherical	[220]
<i>Rhodospseudomonas palustris</i>	CdS	8.01	Spherical	[221]
<i>E. coli</i>	CdS	2–5	Spherical	[222]

Table 3 (continued)

Extract type	Photocatalyst	Size	Shape or application	Refs.
Lemon leaf extract	ZnO-CT		97% Congo Red removal	[223]
<i>Moringa oleifera</i> peel	CeO ₂	40	Spherical	[224]
<i>Prosopis farcta</i> aerial	CeO ₂	30	Uniformly and spherically shaped	[225]
<i>Salvia macrocephalon</i> Boiss. seed	CeO ₂	20–47	Spherical	[226]
Mangrove leaves	TiO ₂	3	Spherical	[227]
<i>Aspergillus flavus</i> TFR7	TiO ₂	12–15	Spherical	[228]
Wheat leaf extract	ZnO	12–37	cubic	[229]
<i>Garcinia xanthochymus</i> fruit	ZnO	20–30	Spherical shape; spongy cave-like structures; crystalline; hexagonal wurtzite	[230]
<i>Trianthema portulacastrum</i>	ZnO	25–90	Crystalline	[231]
<i>Citrus limon</i> , <i>Vitis vinifera</i> , and <i>Cucumis sativus</i> peel	Fe ₃ O ₄	8–12	Spherical and polyhedral shape, inverse cubic spinel structure	[232]
<i>Rubus glaucus</i> Benth. leaf	Fe ₃ O ₄	40–70	Aggregated, spherical	[186]
<i>Syzygium cumini</i>	TiO ₂		Spherical, 83% Pb(II) removal	[233]
<i>Citrus limon</i>	Fe ₃ O ₄		99%, 46% and 48% Pb(II), Cd(II), and As(III) removal	[234]
Mint leaves and orange peels	CuO		Spherical, Qm 89 mg/g and 55 mg/g for Pb(II) and Ni(II)	[235]
<i>Punica granatum</i>	NiFe		77% of tetracycline	[236]
<i>Pseudomonas aeruginosa</i>	ZrO ₂		Qm 526.32 mg/g of tetracycline	[237]
<i>Euphorbia polygonifolia</i>	Fe ₃ O ₄ @CuO		89%, 94% and 96% metronidazole, ciprofloxacin, and cephalixin removal	[238]
<i>Abutilon indicum</i>	MnO		Spherical, 11.5% Cr(IV) removal	[239]
<i>Aspergillus tubingensis</i>	Fe ₂ O ₃		Spherical, 98.0037% Pb(II), 96.4502% Ni(II), 92.1984% Cu(II), and 93.9913% Zn(II)	[240]

multicellular (e.g., *Chlorella*) (e.g., brown algae). In the same way that yeasts have a limited number of research reports, so does this topic. Algae-based NP preparation is a relatively new field of study [21]. For the production of ZnO NPs, the green microalga *Chlamydomonas reinhardtii* has been used. Fast production of ZnO nanoflowers was described. The photocatalytic activity of these nanoflowers was demonstrated in the presence of sunlight. After 2 h, the photocatalytic effectiveness was found to be 90% [178].

5.2 Green Syntheses of Novel Photocatalysts by Using Plant Extracts

The green synthesis of novel photocatalysts with the help of microorganisms has been studied extensively during the last few decades. The biggest disadvantage of the greener approach to microbial NP synthesis is the maintenance and procurement of microbial strain cultures. Furthermore, proper and careful treatment of human pathogenic bacteria is critical. In this case, any carelessness could result in infection and disease. As a result of its virulence, plant extract-mediated NP synthesis has an advantage over microbial synthesis [179]. Plant-assisted photocatalyst synthesis has been shown to be easy and superior to microorganism-assisted synthesis because it does not require the preservation of microbial cultures. Plant extracts have already been shown to decrease and stabilize a variety of metal cations into stable NPs. Many organic compounds found in plant extracts, such as glucose, fructose, water-soluble hydrocarbons, proteins, and other bioactive substances, can be utilized to reduce and stabilize single and multiple metal cations to NPs in a “one-pot” manufacturing process [120]. Many research groups have already investigated green synthesis pathways for metal NP manufacturing from plant extracts (leaves, flowers, roots, seeds, etc.), highlighting their potential applications [180–182]. Elango et al. also demonstrated that a methanolic extract of *Persea americana* (avocado) seed may be used to make tin oxide (SnO₂) NPs. Initially, the fabrication of SnO₂ NPs was confirmed [183].

Ultraviolet–visible (UV–Vis) spectroscopy has also been used in this field. The degradation of phenolsulfonphthalein dye was used to measure the photocatalytic activity of SnO₂ NPs. The SPR band at 426 nm with a clear surface plasmon resonance was used to determine the appropriate dye degradation period [183]. In another study, root bark extracts of *Catunaregam spinosa* were used to obtain stable spherical tin oxide NPs (SnO₂ NPs) with an average size of 47 ± 2 nm. The presence of bioactive chemicals in the extract during contact was confirmed by X-ray diffraction (XRD) spectrum analysis and FTIR analysis. The breakdown of Congo Red in a multilamp photoreactor with 92% irradiation was used to measure the photocatalytic activity of the NPs. An initial degradation rate of 0.0952 min^{-1} and pseudo-first-order kinetics were observed in the Congo Red decay [184]. Surendra and Roopan used *Moringa oleifera* peel extract and microwave irradiation to obtain green cerium oxide NPs (CeO₂ NPs). CeO₂ NPs were characterized by UV–Vis spectroscopy, XRD analysis, FTIR spectroscopy, and high-resolution transmission electron microscopy (HRTEM). These CeO₂ NPs also exhibited antibacterial and photocatalytic properties. Gram-negative bacteria (*Escherichia coli*) were more

resistant to CeO₂ NPs than Gram-positive bacteria (*Staphylococcus aureus*). The photodegradation efficiency of CeO₂ NPs was measured using a Heber multilamp photoreactor with Crystal Violet dye. CeO₂ NPs were found to have a maximum catalytic effectiveness of 97.5% [185]. Kumar et al. investigated the green synthesis of magnetite NPs (Fe₃O₄ NPs) using Andean blackberry leaf extract. XRD analysis, transmission electron microscopy (TEM), FTIR spectroscopy, dynamic light scattering (DLS) measurements, and thermogravimetric (TG) techniques were used to investigate the features of the NPs such as their crystallinity and shape, as well as surface parameters. The NPs were 94% metal and 6% capping ligand, according to the TG analysis. Standard pollutants Congo Red (CR), Methylene Blue (MB), and Methyl Orange (MO) were degraded in the presence of sunlight to test the photoactivity of the Fe₃O₄ NPs. The photodegradation of the dyes was also found to be linked to the in situ production of ROS, such as the hydroxyl radical (OH·), superoxide radical (O₂·), and hydrogen peroxide (H₂O₂) [186]. Bishnoi et al. also showed that *Cynometra ramiflora* fruit extract may be used to make magnetic iron oxide NPs (MIO NPs) in a stable manner. The breakdown of MB dye by sunlight irradiation was used to test the photocatalytic activity of the green-produced NPs. Under sunlight illumination, improved production of OH and faster decolorization of MB were achieved thanks to the large surface area of the MIO NPs [187]. Naik et al. employed aqueous *Cinnamomum tamala* leaf extract as a reducing/capping reagent for the manufacture of Au/TiO₂ nanocomposite through a more environmentally friendly process. The improved nanocomposite showed better degradation of Methyl Orange (MO) dye than Degussa P-25 TiO₂ under solar irradiation [188]. Rostami-Vartooni et al. [189] examined the synthesis of Ag/TiO₂ nanocomposite in another study. As a reducing and stabilizing agent, they employed *Carpobrotus acinaciformis* leaf and flower extract. XRD analysis and field emission scanning electron microscopy (FE-SEM) were used to examine the morphology of the Ag/TiO₂ nanocomposite. The degradation of two distinct dyes was used to measure the photocatalytic activity of the Ag/TiO₂ nanocomposite. The photocatalytic activity of the Au/TiO₂ nanocomposite remained constant after four cycles, according to the researchers [189]. *Azadirachta indica* leaf extract, which is rich in bioactive compounds, was shown by Sankar et al. to be useful in the production of titanium dioxide NPs. It was found that the average particle size of these NPs was 124 nm. Under bright sunlight, photocatalytic degradation was carried out, and the photocatalyst demonstrated degradation activity [190]. For the manufacture of titanium dioxide (TiO₂) NPs, reducing and capping agents can be made from the dried leaves of the plant *Jatropha curcas* L., which are rich in bioactive compounds such as tannins. Under sunlight, the green-produced TiO₂ NPs were used to photocatalytically reduce real tannery wastewater. The reduction of chemical oxygen demand (COD) and Cr⁺⁶ was determined to be 82.26% and 76.48%, respectively [191].

Rambutan (*Nephelium lappaceum* L.) fruit extract can also be utilized to biosynthesize stable ZnO NPs with diameters between 25 and 40 nm, according to Karan and Samuel Selvakumar. The degradation of Methyl Orange (MO) dye under

artificial UV irradiation was used to measure the photocatalytic activity of ZnO NPs. The decolorization efficiency was found to be 83.99% after 120 min of illumination. COD values were used to measure the mineralization efficiency, and after 120 min of UV light, significantly lower COD values were observed when applying the ZnO NPs synthesized using biosynthetic methods [192]. Another work used dried *Camellia sinensis* leaf extract to make zinc oxide NPs from zinc nitrate solution via a “one-pot” technique. The degradation efficiency of the produced zinc oxide NPs was higher than that of commercially available zinc oxide NPs [193].

ZnO NPs can also be made from the latex of *Carica papaya* milk (CPM) [194]. Nanoflowers, agglomerated nanobuds, agglomerated prismatic tips, nanobuds, and prismatic tips were among the five nanostructures created. Furthermore, the produced ZnO nanoflowers exhibited superior antibacterial action against *Pseudomonas aeruginosa* and *Staphylococcus aureus*. FTIR spectroscopy, SEM, transmission electron microscopy (TEM), and HRTEM were used to analyze the ZnO nanoflowers. As a result of its small particle size, the photocatalytic activity of the ZnO nanoflowers was increased. The usefulness of the ethanol extract of *Mimosa pudica* leaves has been demonstrated in several investigations, and coffee powder has also been employed to synthesize ZnO NPs. Because of its larger crystallite size, the ZnO NPs made from *Mimosa pudica* leaf extract had lower bandgap energy [195]. Fowsiya et al. [196] recently described a simple method for phytosynthesis of ZnO NPs using *Carissa edulis* fruit extract (*C. edulis*). The production of ZnO NPs is illustrated by the surface plasmon resonance (SPR) at about 358 nm, according to the authors. Decolorization of Congo Red was performed in a photoreactor, showing a most efficient rate constant (k) of 0.4947, achieving 97% color removed. *Tabernaemontana divaricata* green leaf extract includes flavonoids, steroids, terpenoids, phenolic acids, phenylpropanoids, and enzymes, according to Raja et al. [197], and aqueous extract was employed for the environmentally friendly manufacture of zinc oxide NPs (ZnO NPs). The antibacterial activity of ZnO NPs was investigated against three bacterial strains: *E. coli*, *Salmonella paratyphi*, and *Staphylococcus aureus*. The antibacterial activity of ZnO NPs against *S. paratyphi* was lower. Methylene Blue (MB) decolorization under sunlight was examined to determine the photocatalytic activity of the generated ZnO NPs, taking 90 min to complete. For greener production of ZnO NPs, *Moringa oleifera* natural extract was employed by Archana et al. [198], and the average particle size was found to be between 100 and 200 nm. These NPs were used to generate hydrogen via photocatalysis. The crystalline structure of ZnO NPs was confirmed by XRD analysis and Raman investigation. Vidya et al. [199] demonstrated green synthesis of zinc oxide (ZnO) NPs utilizing *Artocarpus heterophyllus* leaf (jackfruit) extract. The produced ZnO NPs had a hexagonal wurtzite-like shape with particle size of 15–25 nm, according to TEM investigation. This approach produces ZnO NPs with a high photodegradation efficiency (> 80% in 1 h) against Rose Bengal dye. Langmuir–Hinshelwood kinetics were found to be responsible for the degradation of the Rose Bengal dye.

6 Environmental Applications of Photocatalysis

The main applications of photocatalytic phenomena are related to the following processes:

- **Air treatment:** the elimination of ethylene from fruits and vegetables during storage, air stripping of soil for photocatalytic treatment, cleaning of indoor and outdoor air and off-gas emissions, odor elimination, etc.
- **Water treatment:** Digestion and purification of effluent for use in bioreactors and other processes that produce usable water, etc.
- **Active surfaces:** Degradable or antifog materials that can sterilize or sterilize themselves (metals, ceramics and tiles, paints, paper, concrete and cement, glass, textiles, plastics, etc.)
- **Green chemistry:** Photocatalyzed chemical production processes that are more environmentally and economically beneficial
- **Energy conversion:** Water splitting to generate hydrogen gas, or photosynthesis to reduce carbon dioxide gas

6.1 Air and Water Treatment

Photocatalytic reactions require irradiation to begin the reaction. A suitable radiation source is therefore required for photocatalytic reactors; this can be either artificial or natural. A few examples of manmade sources include arc and incandescent lamps, fluorescent lights, lasers, and light-emitting diodes (LEDs). The radiation from these devices can be focused or redirected with the help of reflectors or fiber optics. Reflectors of various types, materials, and concentration ratios can be used to collect solar radiation, or it can be captured directly by the reactor using this technique [241, 242]. It is possible to categorize photoreactor designs for water and air purification based on the radiation characteristics (solar or artificial, concentrated or not), catalyst dispersion (immobilized in various substrates or suspended in solution), reactor geometry (flat plate, parallel plate, U-shaped, fountain, etc.), and operation mode. Many photoreactor designs for water and air purification have been proposed in scientific literature and patents (batch or continuous). Using the kinetic, mass transfer, and radiative transfer equations (RTEs), a simplified or rigorous mathematical model for the photoreactor can be developed following the selection of the photocatalyst and radiation source [243].

Photodegradation rates (r) for chemical contaminants in water and gas phases are related to the fraction of covered surface (Eq. 15) according to the Langmuir–Hinshelwood (L–H) kinetic equation (Eq. 15).

$$r = -\frac{dC}{dt} = \frac{kKC}{1 + KC}, \quad (15)$$

where k is the rate constant, K is the pollutant adsorption constant, and C is the pollutant concentration. It is generally accepted, however, that the rate constants and orders established using this kinetic model are only apparent. Recent years have seen the development of alternative kinetic models such as the direct–indirect

(D–I) model [244], in which the kinetic constants are characterized in terms of the sequence of main events happening during the photocatalytic processes. All of these factors, along with the radiation intensity and wavelength distribution, the type and concentration of pollutants, flow rate, characteristics (turbidity, pH, ionic strength, and dissolved oxygen) of the treated air or water, properties (crystallinity, porosity, doping, loading, etc.) of the catalyst, and reactor design impact on the efficiency and selectivity of the system. The temperature should have little effect on the lamp's performance because of the photonic activation of the process; however, high temperatures may favor charge carrier recombination and disfavor pollutant adsorption. Each application must first be tested in the laboratory because comparing and scaling up are extremely difficult tasks.

The deployment of effective, cost-effective, and environmentally friendly water treatment technologies is in great demand, fueled by the world's rising population and more stringent legislation. There is a considerable possibility that heterogeneous photocatalysis, either alone or in conjunction with other processes, could improve current technological options significantly. Considering that microorganisms are the primary source of contamination in drinking water, disinfection is an important photocatalytic technique for this application. Meanwhile, organic materials as well as trace pollutants from medications, insecticides, and personal care products are found in wastewater. Heavy metals or organic compounds may also be present in industrial wastewater. Insecticides such as aldrin, dichlorvos, and lindan (as well as chloroform and carbon tetrachloride, trichloroethylene, and chlorobenzene) and formaldehyde (as well as formaldehyde, phenol, and methylbenzene) are among the most common pollutants. Degradation mechanisms for a few of these have been discovered [245], but the many factors that influence such photocatalytic processes, as well as the lack of standardization in photocatalytic processes, often lead to conflicting conclusions by different researchers.

Continuous flow tubular reactors with TiO₂ suspensions and nonconcentrating solar compound parabolic collectors (CPC) are used in this experiment [246], and are the most extensively used for aqueous phase photocatalytic reactions. For commercialization, it is necessary to recover the catalyst (e.g., via sedimentation or filtering), although powdered TiO₂ dispersions are used in most water treatment research studies [247]. The use of titania immobilized on a variety of supports, such as adsorbent substrates, and the design of reactors that maintain high efficiency despite the reduced catalyst surface area and mass transfer limits in immobilized systems necessitate a great deal of effort. Reactors utilizing hybrid membranes and photocatalysis [67] and recoverable magnetic photocatalytic particles are promising solutions [248]. The impact of various operational parameters has already been studied in several books and reviews [67, 245]. The performance of aqueous photocatalytic systems is heavily influenced by the pH of the water, in part because of the low adsorption of contaminants owing to water saturation. The neutral surface charge of TiO₂ (point of zero charge, PZC) (pH range of 4.5–7.0) results in no interaction with polar substances, such as water.

The low solubility of oxygen (and thus the need for aeration), radiation absorption in turbid waters, or the presence of water natural components that act as scavengers. Additionally, the kinetics and costs, as well as the suitability of this method for

water treatment, are governed by reactive species such as carbonates or other inorganic anions [249]. One of the most significant disadvantages of TiO_2 photocatalysis, as with other advanced oxidation technologies (AOTs), is their relatively high operating costs compared with traditional biological treatments, particularly the slow kinetics compared with the homogeneous photo-Fenton reaction, which makes the latter more appealing to the scientific community despite the chemical consumption. As a result, heterogeneous photocatalytic water purification systems currently focus on the treatment of non-biodegradable wastewater and the use of solar radiation, particularly in remote areas and developing countries, or the combination of other physical or chemical operations to achieve a synergistic effect. Biological treatments, membrane reactors, and physical adsorption do not affect the photocatalytic efficiency, but they do improve the overall process when used in conjunction with ultrasonic irradiation, a photo-Fenton reaction, ozonation, or electrochemical treatment [250, 251]. Since it reacts with water-soluble contaminants that are not biodegradable, photocatalysis is currently a popular pretreatment method before biological water treatment.

6.2 Self-Cleaning Materials

The air-cleaning and self-cleaning, self-sterilizing, and antifogging properties of TiO_2 -containing materials have sparked interest from the scientific community as well as the construction and vehicle sectors. However, these materials are usually optimized for their primary function. Material that is self-cleaning but lacks the adsorption capacity needed for air treatment applications is preferable to material that is smooth, such as the thin coating on a window. The self-cleaning properties of TiO_2 surfaces can be attributed to a combination of reasons. Adsorption sites for particles such as soot and grime can be removed through photocatalytic elimination of organic deposits as well as the simultaneous inactivation and mineralization of surface microorganisms (self-sterilizing properties). Second, photoinduced superhydrophilicity prevents water from forming surface droplets; instead, when exposed to light, a homogeneous thin water layer covers the surface beneath the dirt, allowing dirt to be washed away readily. Superhydrophilicity also prevents fogging since water attempts to run off the surface (fogging occurs at water contact angles greater than 200°). Metals can be protected against corrosion by using TiO_2 coatings, which introduce electrons into the metal, or the heat transfer rate can be increased on superhydrophilic surfaces, which reduces water usage while also improving heat transmission. For example, the latent heat of evaporation is employed to cool buildings using falling film evaporators and passive cooling systems based on this effect [252]. Nanofunctionalized thin films over glasses have recently been shown to have antireflective and photocatalytic characteristics compatible to low-refractive-index nanoporous silica and high-refractive-index titania in low-refractive-index nanoporous silica–titania [253].

6.3 Green Materials in Fuel Cells

Fuels produced using green methods or chemistry are a critical source for power generation today. The limited availability of existing fuels, such as petroleum products, results in higher environmental pollution and costs. It is thus critical to find a new source of energy materials that is ecologically benign, low cost, and readily available in Nature. Green photocatalysts enable a process that uses light energy and natural resources to produce fossil fuels. Biomass can be used to produce hydrogen fuels and biodiesel, for example [254, 255]. Hydrogen fuel is one of the zero-carbon transportation fuels that can be made from biomass, but it has limitations in terms of large-scale manufacturing [255]. This type of fuel, which is made from natural resources, can help to reduce greenhouse-gas emissions and enhance the quality of the air we breathe. Nanotechnology is the most effective technique for transferring this approach into the real world [256–258]. This provides a fantastic platform for research organizations to use nanotechnology to develop novel renewable energy materials. Li-ion batteries, flow batteries, supercapacitors, fuel cells, solar cells, and fire- and heat-retardant insulation applications are among the areas where nanotechnology plays an important role in alternative energy production, according to recent studies. Nanotechnology offers a more efficient method of producing solar cells. Essentially, the fabrication process is solely reliant on the absorption of light and the conveyance of charge carriers, both of which are easily accessible and have a low production cost [154]. In dye-sensitized solar cells, coloring compounds taken from plants are utilized for sensitization in dye-sensitized solar cells (DSSCs). The coloring chemicals aid in the absorption of a wider range of light, increasing the efficiency of solar cells. Hydrogen fuels are created by converting biomass, which uses 35% less energy than the electricity required to go 400 km in a battery-powered electric car.

6.4 Green Photocatalytic Disinfection of Water

Water is a necessity for human survival. In our ecology, the availability of fresh, pure water is quite restricted [259]. The majority of water sources have been polluted as a result of urbanization and industry. Textiles, tanneries, and pharmaceuticals are among the businesses that dump waste or byproducts into water bodies. Solar energy is a plentiful natural resource that is freely available on the Earth's surface, and the collective radiation of sunlight can eradicate harmful bacteria in water bodies. Various process characteristics, such as light intensity, incoming light temperature, and pathogen type, can directly inhibit the photocatalytic efficiency of solar disinfection (SODIS) processes [260]. Heterogeneous photocatalysis is the most viable method for effectively killing microorganisms. Clasen et al. [261] reported on a cost-effective strategy for preventing diarrhea in the home. They concluded that the most cost-efficient and effective solar disinfection technology is a household-based water purification system. Even though it is slightly more expensive than chlorination, it has a higher overall disinfection efficacy than SODIS [260]. By immobilizing the photocatalyst under UV irradiation, the water purification process can be carried

out in aqueous solution [262]. The disinfection level of the aqueous solution should be measured before and after light exposure at regular intervals. TiO_2 photocatalysts outperform UVA therapy alone in terms of water disinfection efficiency. Alrousan et al. used two different configurations with and without a photocatalyst (TiO_2) to demonstrate solar light-induced photocatalytic (SPC-DIS) and solar disinfection (SODIS) of *E. coli*-polluted water [263]. According to recent scientific findings, the most promising strategy for achieving effective catalytic activity under visible light irradiation is doping to achieve metal ion inclusion in the host material [256, 264]. However, research on microorganism disinfection is sparse, and reported publications are likewise few when compared with papers on photocatalytic disinfection of organic pollutants.

6.5 Photoelectrochemical H_2 Production via Water Splitting

It is widely known that using an appropriate semiconductor photocatalyst can enable effective conversion of solar energy to chemical energy for the generation of clean energy [265]. Thus, using semiconductor photocatalysts with efficient nanostructures that have a high surface-to-volume ratio and a high capacity for light absorption, hydrogen can be created by photoelectrochemical (PEC) water splitting. The two half-reactions that make up a typical PEC cell are (a) the oxygen evolution reaction (OER), which typically takes place on an *n*-type semiconductor as a photoanode, and (b) the hydrogen evolution reaction (HER), which typically takes place on a cathode as a counterelectrode. By evaluating various nanostructured semiconductor photocatalysts, several researchers are making considerable efforts to increase the efficiency of the hydrogen generation rate under solar irradiation [265].

6.6 Photocatalytic CO_2 Reduction

As of 2019, it was stated that the significant use of fossil fuels caused enormous carbon emissions, with an atmospheric concentration exceeding 400 ppm. A significant quantity of CO_2 is released into the environment as a result of the excessive use of fossil fuels (e.g., petroleum, gas, and coal) [265]. Around 76% of yearly greenhouse gas (GHG) emissions are attributed to the release of CO_2 , which has serious negative effects on the environment and human health by contributing to climate change, ocean acidification, and ocean warming [265]. By using photocatalytic technology to convert CO_2 into valuable small-molecule chemical products or energy sources (such as CO , CH_4 , HCOOH , and other chemicals), the energy crisis and these serious ecological problems could be resolved. The conversion of GHGs, such as CO_2 , into useful goods and the reduction of its disastrous release have both been the subject of extensive investigation by several scientists. As a consequence of such development, environmental issues including climatic effects such as ecological degradation, seawater acidification, and the rise in ocean levels could be lessened [265, 266].

6.7 Photocatalytic Dye/Drug Degradation

According to a World Bank assessment, the textile and dyeing sectors are responsible for between 17% and 20% of water contamination [267]. With an annual worldwide output of 8×10^5 tons of dyes, of which around 200,000 tons are textiles and dyes, the textile, leather, food, and paper sectors are principally responsible for manufacturing dye wastewater, according to a newly published report [268]. Numerous synthetic dyes used in textiles, including cationic dyes such as Safranin O, Rhodamine B, Malachite Green, Rhodamine 6G, Methylene Blue, and Crystal Violet, and anionic dyes such as Eosin Y, Eriochrome Black T, Phenol Red, Methylene Orange, and Congo Red, are toxic and harmful organic contaminants that can hinder the photosynthesis process of aquatic plants and pose a threat to the other organic wastes that are damaging to society and the environment are created by the chemical and pharmaceutical industries. To meet the needs of modern lifestyles and expanded healthcare, pharmaceutical and personal care products (PPCPs) have been produced and increasingly used during the course of the last few decades [272]. There are over 3000 commonly used medications, and their use is still increasing globally, according to the European Union market [273]. According to a recent analysis, the amount of antibiotics used globally is estimated to be between 100,000 and 200,000 metric tons. Of the antibiotics used, 70–90% remain chemically unchanged or are eliminated from the body as active metabolites [274]. In addition, the coronavirus disease 2019 (COVID-19) epidemic has considerably expanded PPCP production and usage worldwide in recent years. According to the People's Republic of China's National Health Commission, the usage of antiviral and antibiotic medications increased dramatically during the pandemic [275]. Water can contain pharmaceutical pollutants in amounts ranging from ng/L^{-1} to $\mu\text{g/L}^{-1}$. Even at these low concentration levels, they can represent a major hazard to the health of living creatures owing to their chemical and physical characteristics [276]. Numerous attempts have been made to develop highly effective semiconductor-based photocatalysts to photodegrade dye and pharmaceutical pollutants owing to the serious issues associated with dye and pharmaceutical pollutants in water, as well as to the significant advantages of photocatalysis processes in removing harmful pollutants from water.

7 Simultaneous Photocatalysis

Significant effort and studies have been devoted to the use of suitable semiconducting photocatalysts in a variety of crucial chemical reactions, e.g., for wastewater treatment, H_2 generation, CO_2 reduction, organic transformations, N_2 photofixation, biomass conversion to valuable products, and heterogeneous photocatalytic reactions, over the past 10 years [265]. These processes are well known in traditional photocatalytic research, and they take place under controlled conditions and are each studied independently in literature. The simultaneous use of two or more functionalities in a single photocatalytic device, however, is a more recent creative strategy [265]. The difficult aspect is that merging two functions into a single photocatalytic system necessitates a novel approach to semiconductor photocatalyst design,

control, and engineering with specific properties for each use in a given environment. The groundbreaking study of Kim et al. [277] on simultaneous H₂ generation and phenolic compound degradation by employing a TiO₂ surface decorated with platinum nanoparticles and fluorine atoms as a photocatalyst explored this idea of dual-purpose photocatalysis. They achieved full mineralization of organic molecules and found anoxic 4-chlorophenol degradation, which was accompanied by H₂ generation. Since a suitable photocatalyst characteristic is needed for each operation, conducting two or more types of applications over a single photocatalyst at once is the main problem. As a result, the best approach is to build and employ a unique photocatalyst in at least two distinct concurrent applications. For instance, two-dimensional (2D) semiconductors such as graphene oxide (GO), reduced graphene oxide (rGO), and MXenes and their hybrid combinations can be used to concurrently generate H₂ and degrade pollutants. Zinc porphyrin metal–organic frameworks noncovalently attached to graphene oxide (SURMOF/GO) were created by Nugmanova et al. [278] in Pickering emulsions, and their photocatalytic activity during the photodegradation of Rhodamine 6G and 1,5-dihydroxynaphthalene was examined. Using methyl viologen as a sacrificial electron acceptor, Nikoloudakis et al. [279] created a covalently connected nickel(II) porphyrin–ruthenium(II) tris(bipyridyl) dyad for a photocatalytic water oxidation process in dimethylformamide (DMF).

8 AI-Assisted Photocatalyst Design

The discovery of electrocatalysts [269] and photocatalysts [280] has been revolutionized recently by the development of artificial intelligence (AI) and machine learning (ML) approaches. The term “machine learning” is frequently used to describe processes in which a simulation of the relationship between specified reference or input qualities and the parameters of the output to be predicted from the input is “learned” using a suitable training dataset. A large dataset of 10,560 data points from 584 experiments described in 180 scholarly papers about photoelectrochemical water splitting over *n*-type semiconductors was analyzed by Oral et al. [281] using such machine learning techniques. To establish a relationship between the photocurrent density and 33 descriptors, including the type of electrode, preparation techniques, light irradiation condition, and electrolyte solution, the researchers used a predictive model created by random forest statistics to find patterns in the data. With a root-mean-square error of validation and testing of 0.24 and 0.27, respectively, the obtained bandgap of the electrode was astonishingly excellent. Generally speaking, a more comprehensive training dataset is also needed as an ML model’s complexity rises. Such models may infer catalyst activity without doing real trials or simulating conditions, since they have been trained. Using predictive ML models instead of more traditional experimental or computational approaches might be a cost-effective way to determine the photocatalytic activity of a catalyst on the basis of its parameters. By using this method, the time and resources needed to ascertain the photocatalytic activity may be greatly reduced. Additionally, one method for working with a small quantity of data is to combine domain expertise with data-driven ML model training. Numerous types of photocatalysis domain knowledge are offered

from the viewpoint of heterogeneous catalysis, leading to the most recent data-driven machine learning advancements. As a result, the need for tests and simulations decreases through the training of precise prediction models, enabling effective photocatalyst screening. The use of ML to provide trustworthy predictions about the choice of dopants for PEC systems with exceptional performance seems promising. A useful technique for identifying previously obscure links is the examination of correlations between numerous dopant characteristics and the photoelectrochemical performance of doped photoelectrodes [282]. Wang et al. [282] successfully built an ML model that can predict the effects of 17 metal dopants on hematite (Fe_2O_3), a typical photoelectrode material. A methodology for analyzing the influence of dopants for their underlying structural properties, as recorded in database S, is provided by Wang et al. [282]. A total of 11 descriptors are included in the database S, including atomic number (N), ionic radius (r_i), atomic radius (r_a), single-molecule bond covalent radius (r_c), chemical valence (Z), M–O bond formation enthalpy based on metal and oxygen, electronegativity (x), and melting temperature of pure metal (T_m). Furthermore, utilizing different operational variables as input, scientists have employed a variety of ML techniques to forecast pollution removal using photocatalytic reactions [265].

9 Conclusions and Future Perspective Directions

Because of the unique features of nanomaterials, nanotechnology offers the ability to store solar energy and remove organic contaminants from the environment. Artificial photosynthesis systems have a lot of potential. To meet current environmental concerns, green, accessible, and safe techniques for generating such NPs are required. A fast reaction process, low temperature, and limited use of chemicals are all important elements of green or biosynthetic solutions based on biomass feedstock. We can create light-harvesting assemblies, new methods for synthesizing fuels, and instruments to synthesize innovative functional materials for solar cells, water-splitting units, pollution control devices, and more by emulating photoactive green nanomaterials found in Nature. To create metallic NPs without the use of dangerous chemicals, a practical and environmentally friendly approach must be devised. As discussed in this review, researchers around the world are already working on new techniques to make metallic NPs. As a result, the more environmentally friendly production of metallic NPs is gaining a competitive advantage over alternative synthesis methods. This review also covers the use of ecologically friendly synthesis of metallic NPs that also serve as photocatalysts, using a variety of species such as plants, bacteria, fungi, and algae. Even if there has been a lot of progress, the following problems still need to be solved in the future: (1) there is a chance to create new photocatalytic materials with increased effectiveness, selectivity, and reusability by the synthesis of novel materials or modification of existing materials; (2) one novel method for enhancing the photocatalytic performance of semiconductors in a variety of applications is to optimize the semiconductor structure for the creation of flexible and more stable photocatalysts with self-cleaning and flame-resistance qualities; (3) from the economical point of view, it is promising to create photocatalytic systems that are active in the presence of natural sunlight, to

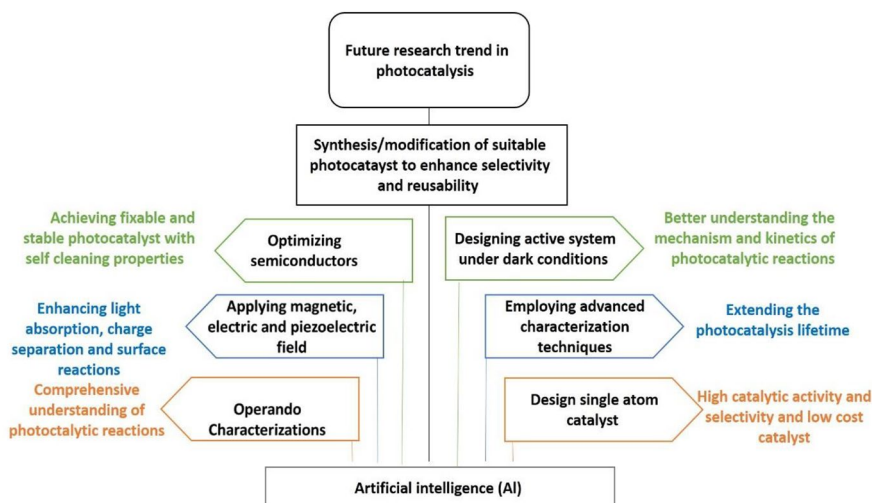


Fig. 16 A schematic illustration of future research direction regarding photocatalytic processes [265]

significantly increase the photocatalyst lifespan; (4) enhancing photocatalytic reactions by using different types of external field, such as magnetic, electric, and piezoelectric fields, might result in the creation of more effective photocatalysts by improving light absorption, charge separation, and surface reactions; (5) to create more efficient photocatalytic systems for the generation of clean energy and environmental remediation, enhanced characterization investigations might also be carried out to get a better knowledge of the kinetics and processes of the photocatalytic reactions. Designing single-atom catalysts to achieve high catalytic activity and selectivity while lowering practical costs is another important future idea that has gained a lot of media interest lately. The major factor increasing the atomic efficiency of metals in these systems is the isolation of scattered atoms or coordination atoms with surface atoms on a suitable substrate. Last but not least, operando characterization, or simultaneous online examination of photocatalyst performance using in situ imaging techniques such as scanning tunneling microscopy while functioning under actual conditions, aids in gaining a thorough knowledge of the photocatalytic reaction. Future research directions for a photocatalytic process are shown in Fig. 16. As a result, more study is needed to improve present processes and methodologies, which will help the research community and the general public in the future while also posing problems.

Author Contributions MAH: writing—original draft preparation; data creation. MAH: conceptualization, methodology; investigation. MRE, MAE, SR, AE, MAH, and V-CN: writing—review and editing, investigation, and visualization. AEN: supervision.

Funding Open access funding provided by The Science, Technology & Innovation Funding Authority (STDF) in cooperation with The Egyptian Knowledge Bank (EKB). This research received no external funding.

Data availability The datasets used in this review are available upon request from the corresponding author of the paper.

Declarations

Conflict of interest The authors declare no conflict of interest.

Open Access This article is licensed under a Creative Commons Attribution 4.0 International License, which permits use, sharing, adaptation, distribution and reproduction in any medium or format, as long as you give appropriate credit to the original author(s) and the source, provide a link to the Creative Commons licence, and indicate if changes were made. The images or other third party material in this article are included in the article's Creative Commons licence, unless indicated otherwise in a credit line to the material. If material is not included in the article's Creative Commons licence and your intended use is not permitted by statutory regulation or exceeds the permitted use, you will need to obtain permission directly from the copyright holder. To view a copy of this licence, visit <http://creativecommons.org/licenses/by/4.0/>.

References

1. Saravanan A, Kumar PS, Jeevanantham S, Anubha M, Jayashree S (2022) Degradation of toxic agrochemicals and pharmaceutical pollutants: Effective and alternative approaches toward photocatalysis. *Environ Pollut*. <https://doi.org/10.1016/j.envpol.2022.118844>
2. Uribe-López MC, Hidalgo-López MC, López-González R, Frías-Márquez DM, Núñez-Nogueira G, Hernández-Castillo D, Alvarez-Lemus MA (2021) Photocatalytic activity of ZnO nanoparticles and the role of the synthesis method on their physical and chemical properties. *J Photochem Photobiol, A* 404:112866. <https://doi.org/10.1016/j.jphotochem.2020.112866>
3. Spinelli P, Ferry VE, Van de Groep J, Van Lare M, Verschuuren MA, Schropp REI, Atwater HA, Polman A (2012) Plasmonic light trapping in thin-film Si solar cells. *J Opt* 14(2):024002. <https://doi.org/10.1088/2040-8978/14/2/024002>
4. Sahu K, Bisht A, Khan SA, Sulania I, Singhal R, Pandey A, Mohapatra S (2020) Thickness dependent optical, structural, morphological, photocatalytic and catalytic properties of radio frequency magnetron sputtered nanostructured Cu₂O–CuO thin films. *Ceram Int* 46(10):14902–14912. <https://doi.org/10.1016/j.ceramint.2020.03.017>
5. Hassaan, M.A., El Nemr, A. and Ragab, S., 2021a. Green Synthesis and Application of Metal and Metal Oxide Nanoparticles. *Handbook of Nanomaterials and Nanocomposites for Energy and Environmental Applications*, pp.1–27.
6. Hassaan MA, El Nemr A, Elkatory MR, Ragab S, El-Nemr MA, Pantaleo A (2021) Synthesis, characterization, and synergistic effects of modified biochar in combination with α -Fe₂O₃ NPs on biogas production from red algae *Pterocladia capillacea*. *Sustainability* 13(16):9275
7. Hassaan MA, Hosny S, Elkatory MR, Ali RM, Rangreez TA, El Nemr A (2021) Dual action of both green and chemically synthesized zinc oxide nanoparticles: antibacterial activity and removal of Congo red dye. *Desalin Water Treat* 218:423–435. <https://doi.org/10.5004/dwt.2021.26988>
8. Annu AA, Ahmed S (2018) Green synthesis of metal, metal oxide nanoparticles, and their various applications. *Handbook of Ecomaterials 2018*:1–45. https://doi.org/10.1007/978-3-319-68255-6_115
9. Kay A, Cesar I, Grätzel M (2006) New benchmark for water Photooxidation by nanostructured α -Fe₂O₃ films. *J Am Chem Soc* 128(49):15714–15721. <https://doi.org/10.1021/ja064380l>
10. Ma, G., Hisatomi, T. and Domen, K., 2015. Semiconductors for photocatalytic and photoelectrochemical solar water splitting. In *From molecules to materials* (pp. 1–56). Springer, Cham. <https://doi.org/10.1007/978-3-319-13800-81>.
11. Verma LK, Sakhuja M, Son J, Danner AJ, Yang H, Zeng HC, Bhatia CS (2011) Self-cleaning and antireflective packaging glass for solar modules. *Renewable Energy* 36(9):2489–2493. <https://doi.org/10.1016/j.renene.2011.02.017>

12. El Nemr A, Hassaan MA, Elkatory MR, Ragab S, Pantaleo A (2021) Efficiency of Fe₃O₄ nanoparticles with different pretreatments for enhancing biogas yield of macroalgae *Ulva intestinalis* Linnaeus. *Molecules* 26(16):5105
13. Hassaan, M.A., El Nemr, A., El-Zahhar, A.A., Idris, A.M., Alghamdi, M.M., Sahlabji, T. and Said, T.O., 2020a. Degradation mechanism of Direct Red 23 dye by advanced oxidation processes: a comparative study. *Toxin Reviews*, pp.1–10.
14. Hassaan M, El Katory M, Ali RM, El Nemr A (2020) Photocatalytic degradation of reactive black 5 using Photo-Fenton and ZnO nanoparticles under UV irradiation. *Egypt J Chem* 63(4):1443–1459. <https://doi.org/10.21608/EJCHEM.2019.15799.1955>
15. Hassaan MA, Pantaleo A, Santoro F, Elkatory MR, De Mastro G, Sikaily AE, Ragab S, Nemr AE (2020) Techno-Economic Analysis of ZnO Nanoparticles Pretreatments for Biogas Production from Barley Straw. *Energies* 13(19):5001
16. Yin Y, Chen H, Yuan Q (2021) Strain-induced bandgap engineering in C3N nanotubes. *Chem Phys Lett* 768:138390. <https://doi.org/10.1016/j.cplett.2021.138390>
17. Christian P, Von der Kammer F, Baalousha M, Hofmann T (2008) Nanoparticles: structure, properties, preparation and behaviour in environmental media. *Ecotoxicology* 17(5):326–343. <https://doi.org/10.1007/s10646-008-0213-1>
18. Sarath, N.G., Shackira, A.M., El-Serehy, H.A., Hefft, D.I. and Puthur, J.T., 2022. Phytostabilization of arsenic and associated physio-anatomical changes in *Acanthus ilicifolius* L. *Environmental Pollution*, p.118828. <https://doi.org/10.1016/j.envpol.2022.118828>.
19. Salam HA, Sivaraj R, Venkatesh R (2014) Green synthesis and characterization of zinc oxide nanoparticles from *Ocimum basilicum* L. var. *purpurascens* Benth.-*Lamiaceae* leaf extract. *Mater Lett* 131:16–18. <https://doi.org/10.1016/j.matlet.2014.05.033>
20. Miyata T, Tokunaga H, Watanabe K, Ikenaga N, Minami T (2020) Photovoltaic properties of low-damage magnetron-sputtered n-type ZnO thin film/p-type Cu₂O sheet heterojunction solar cells. *Thin Solid Films* 697:137825. <https://doi.org/10.1016/j.tsf.2020.137825>
21. Agarwal H, Kumar SV, Rajeshkumar S (2017) A review on green synthesis of zinc oxide nanoparticles—An eco-friendly approach. *Resource Efficient Technologies* 3(4):406–413. <https://doi.org/10.1016/j.refit.2017.03.002>
22. Chng, L.L., Erathodiyil, N. and Ying, J.Y., 2013. Nanostructured catalysts for organic transformations. *Accounts of chemical research*, 46(8), pp.1825–1837. <https://doi.org/10.1021/ar300197s>
23. Abdel-Aziz R, Ahmed MA, Abdel-Messih MF (2020) A novel UV and visible light driven photocatalyst AgIO₄/ZnO nanoparticles with highly enhanced photocatalytic performance for removal of rhodamine B and indigo carmine dyes. *J Photochem Photobiol, A* 389:112245. <https://doi.org/10.1016/j.jphotochem.2019.112245>
24. Hoffmann MR, Martin ST, Choi W, Bahnemann DW (1995) Environmental applications of semiconductor photocatalysis. *Chem Rev* 95(1):69–96. <https://doi.org/10.1021/cr00033a004>
25. Turchi CS, Ollis DF (1990) Photocatalytic degradation of organic water contaminants: mechanisms involving hydroxyl radical attack. *J Catal* 122(1):178–192. [https://doi.org/10.1016/0021-9517\(90\)90269-P](https://doi.org/10.1016/0021-9517(90)90269-P)
26. Zhang X, Chen YL, Liu RS, Tsai DP (2013) Plasmonic photocatalysis. *Rep Prog Phys* 76(4):046401. <https://doi.org/10.1088/0034-4885/76/4/046401>
27. Mirzaeifard Z, Shariatinia Z, Jourshabani M, Rezaei Darvishi SM (2020) ZnO photocatalyst revisited: effective photocatalytic degradation of emerging contaminants using S-doped ZnO nanoparticles under visible light radiation. *Ind Eng Chem Res* 59(36):15894–15911. <https://doi.org/10.1021/acs.iecr.0c03192>
28. Wang W, Bi J, Wu L, Li Z, Fu X (2009) Hydrothermal synthesis and catalytic performances of a new photocatalyst CaSnO₃ with microcube morphology. *Scripta Mater* 60(3):186–189. <https://doi.org/10.1016/j.scriptamat.2008.10.001>
29. Wang X, Maeda K, Thomas A, Takanabe K, Xin G, Carlsson JM, Domen K, Antonietti M (2009) A metal-free polymeric photocatalyst for hydrogen production from water under visible light. *Nat Mater* 8(1):76–80. <https://doi.org/10.1038/nmat2317>
30. Janani B, Okla MK, Abdel-Maksoud MA, Abdelgawad H, Thomas AM, Raju LL, Al-Qahtani WH, Khan SS (2022) CuO loaded ZnS nanoflower entrapped on PVA-chitosan matrix for boosted visible light photocatalysis for tetracycline degradation and anti-bacterial application. *J Environ Manage* 306:114396. <https://doi.org/10.1016/j.jenvman.2021.114396>
31. Foster R, Ghassemi M, Cota A (2009) *Solar energy: renewable energy and the environment*. CRC Press, New York

32. Prusty JK, Patro SK, Basarkar SS (2016) Concrete using agro-waste as fine aggregate for sustainable built environment—A review. *Int J Sustain Built Environ* 5(2):312–333. <https://doi.org/10.1016/j.ijsbe.2016.06.003>
33. Al-Othman, Z.A., Ali, R. and Naushad, M., 2012. Hexavalent chromium removal from aqueous medium by activated carbon prepared from peanut shell: adsorption kinetics, equilibrium and thermodynamic studies. *Chemical engineering journal*, 184, pp.238–247. <https://doi.org/10.1016/j.cej.2012.01.048>.
34. Ramírez-Rico J, Martínez-Fernandez J, Singh M (2017) Biomorphic ceramics from wood-derived precursors. *Int Mater Rev* 62(8):465–485. <https://doi.org/10.1080/09506608.2017.1354429>
35. Singh, M., Ohji, T. and Asthana, R. eds., 2015a. Green and sustainable manufacturing of advanced material. Elsevier.
36. Singh, M., Ohji, T. and Asthana, R. eds., 2015b. Green and sustainable manufacturing of advanced material. Elsevier.
37. Abas N, Kalair A, Khan N (2015) Review of fossil fuels and future energy technologies. *Futures* 69:31–49. <https://doi.org/10.1016/j.futures.2015.03.003>
38. Bilgili M, Ozbek A, Sahin B, Kahraman A (2015) An overview of renewable electric power capacity and progress in new technologies in the world. *Renew Sustain Energy Rev* 49:323–334. <https://doi.org/10.1016/j.rser.2015.04.148>
39. Ali SH, Giurco D, Arndt N, Nickless E, Brown G, Demetriades A, Durrheim R, Enriquez MA, Kinnaird J, Littleboy A, Meinert LD (2017) Mineral supply for sustainable development requires resource governance. *Nature* 543(7645):367–372. <https://doi.org/10.1038/nature21359>
40. Schandl H, Hatfield-Dodds S, Wiedmann T, Geschke A, Cai Y, West J, Newth D, Baynes T, Lenzen M, Owen A (2016) Decoupling global environmental pressure and economic growth: scenarios for energy use, materials use and carbon emissions. *J Clean Prod* 132:45–56. <https://doi.org/10.1016/j.jclepro.2015.06.100>
41. Priedulena, E. and Hogeforster, M. eds., 2016. Improvement of skills in the green economy through the advanced training programs on cradle to cradle. BoD—Books on Demand.
42. Nozik AJ (1977) Photochemical diodes. *Appl Phys Lett* 30(11):567–569. <https://doi.org/10.1063/1.89262>
43. Bard AJ (1979) Photoelectrochemistry and heterogeneous photo-catalysis at semiconductors. *J Photochem* 10(1):59–75. [https://doi.org/10.1016/0047-2670\(79\)80037-4](https://doi.org/10.1016/0047-2670(79)80037-4)
44. Osterloh FE (2017) Photocatalysis versus photosynthesis: A sensitivity analysis of devices for solar energy conversion and chemical transformations. *ACS Energy Lett* 2(2):445–453
45. Chowdhury, S. and Balasubramanian, R., 2014. Graphene/semiconductor nanocomposites (GSNs) for heterogeneous photocatalytic decolorization of wastewaters contaminated with synthetic dyes: a review. *Applied Catalysis B: Environmental*, 160, pp.307–324. <https://doi.org/10.1016/j.apcatb.2014.05.035>.
46. Bora LV, Mewada RK (2017) Visible/solar light active photocatalysts for organic effluent treatment: Fundamentals, mechanisms and parametric review. *Renew Sustain Energy Rev* 76:1393–1421. <https://doi.org/10.1016/j.rser.2017.01.130>
47. Lems S, Van Der Kooij HJ, De Swaan Arons J (2010) Exergy analyses of the biochemical processes of photosynthesis. *Int J Exergy* 7(3):333–351
48. Whitmarsh, J., 1999. The photosynthetic process. In *Concepts in photobiology* (pp. 11–51). Springer, Dordrecht. https://doi.org/10.1007/978-94-011-4832-0_2.
49. Sayama K, Mukasa K, Abe R, Abe Y, Arakawa H (2002) A new photocatalytic water splitting system under visible light irradiation mimicking a Z-scheme mechanism in photosynthesis. *J Photochem Photobiol A: Chem* 148(1–3):71–77. [https://doi.org/10.1016/S1010-6030\(02\)00070-9](https://doi.org/10.1016/S1010-6030(02)00070-9)
50. Dayan FE, Duke SO, Grossmann K (2010) Herbicides as probes in plant biology. *Weed Sci* 58(3):340–350. <https://doi.org/10.1614/WS-09-092.1>
51. El Nemr A, Helmy ET, Arafa E, Eldafrawy S, Mousa M (2019) Photocatalytic and biological activities of undoped and doped TiO₂ prepared by Green method for water treatment. *J Environ Chem Eng* 7(5):103385
52. Hernández-Ramírez, A, Medina-Ramírez, I., 2015. Semiconducting materials. In *Photocatalytic semiconductors* (pp. 1–40). Springer, Cham. <https://doi.org/10.1007/978-3-319-10999-2>.
53. Djurišić AB, Leung YH, Ng AMC (2014) Strategies for improving the efficiency of semiconductor metal oxide photocatalysis. *Mater Horiz* 1(4):400–410. <https://doi.org/10.1039/c4mh00031e>

54. Hisatomi T, Kubota J, Domen K (2014) Recent advances in semiconductors for photocatalytic and photoelectrochemical water splitting. *Chem Soc Rev* 43(22):7520–7535. <https://doi.org/10.1039/C3CS60378D>
55. Pelizzetti E, Minero C (1994) Metal oxides as photocatalysts for environmental detoxification. *Comments Inorg Chem* 15(5–6):297–337. <https://doi.org/10.1080/02603599408035846>
56. Chan SHS, Yeong Wu, T., Juan, J.C. and Teh, C.Y. (2011) Recent developments of metal oxide semiconductors as photocatalysts in advanced oxidation processes (AOPs) for treatment of dye waste-water. *J Chem Technol Biotechnol* 86(9):1130–1158. <https://doi.org/10.1002/jctb.2636>
57. Ali RM, El Katory M, Hassaan M, Amer K, El Geiheini A (2020) Highly crystalline heterogeneous catalyst synthesis from industrial waste for sustainable biodiesel production. *Egypt J Chem* 63(4):1161–1178
58. Chen, X., Shen, S., Guo, L. and Mao, S.S., 2010. Semiconductor-based photocatalytic hydrogen generation. *Chemical reviews*, 110(11), pp.6503–6570. <https://doi.org/10.1021/cr1001645>.
59. Nie M, Liao J, Cai H, Sun H, Xue Z, Guo P, Wu M (2021) Photocatalytic property of silver enhanced Ag/ZnO composite catalyst. *Chem Phys Lett* 768:138394. <https://doi.org/10.1016/j.cplett.2021.138394>
60. Putri AE, Roza L, Budi S, Umar AA, Fauzia V (2021) Tuning the photocatalytic activity of nano-composite ZnO nanorods by shape-controlling the bimetallic AuAg nanoparticles. *Appl Surf Sci* 536:147847. <https://doi.org/10.1016/j.apsusc.2020.147847>
61. Choudhary S, Sahu K, Bisht A, Satpati B, Mohapatra S (2021) Rapid synthesis of ZnO nanowires and nanoplates with highly enhanced photocatalytic performance. *Appl Surf Sci* 541:148484. <https://doi.org/10.1016/j.apsusc.2020.148484>
62. Ljubas D (2005) Solar photocatalysis—a possible step in drinking water treatment. *Energy* 30(10):1699–1710. <https://doi.org/10.1016/j.energy.2004.11.010>
63. Salah H, Elkatory MR, Fattah MA (2021) Novel zinc-polymer complex with antioxidant activity for industrial lubricating oil. *Fuel* 305:121536. <https://doi.org/10.1016/j.fuel.2021.121536>
64. Mozia, S., 2010. Photocatalytic membrane reactors (PMRs) in water and wastewater treatment. A review. *Separation and purification technology*, 73(2), pp.71–91. <https://doi.org/10.1016/j.seppur.2010.03.021>.
65. Herrmann JM (2010) Photocatalysis fundamentals revisited to avoid several misconceptions. *Appl Catal B* 99(3–4):461–468. <https://doi.org/10.1016/j.apcatb.2010.05.012>
66. Fogler, H.S. and Fogler, S.H., 1999. *Elements of chemical reaction engineering*. Pearson Educación. pp 87.
67. Chong, M.N., Jin, B., Chow, C.W. and Saint, C., 2010. Recent developments in photocatalytic water treatment technology: a review. *Water research*, 44(10), pp.2997–3027. <https://doi.org/10.1016/j.watres.2010.02.039>.
68. Van Gerven T, Mul G, Moulijn J, Stankiewicz A (2007) A review of intensification of photocatalytic processes. *Chem Eng Process* 46(9):781–789. <https://doi.org/10.1016/j.cep.2007.05.012>
69. Konstantinou IK, Albanis TA (2004) TiO₂-assisted photocatalytic degradation of azo dyes in aqueous solution: kinetic and mechanistic investigations: a review. *Appl Catal B* 49(1):1–14. <https://doi.org/10.1016/j.apcatb.2003.11.010>
70. Mondal K, Sharma A (2016) Recent advances in the synthesis and application of photocatalytic metal–metal oxide core–shell nanoparticles for environmental remediation and their recycling process. *RSC Adv* 6(87):83589–83612. <https://doi.org/10.1039/C6RA18102C>
71. Reuterghåd LB, Iangphasuk M (1997) Photocatalytic decolourization of reactive azo dye: A comparison between TiO₂ and us photocatalysis. *Chemosphere* 35(3):585–596. [https://doi.org/10.1016/S00456535\(97\)00122-7](https://doi.org/10.1016/S00456535(97)00122-7)
72. Qamar M, Saquib M, Muneer M (2005) Photocatalytic degradation of two selected dye derivatives, chromotrope 2B and amido black 10B, in aqueous suspensions of titanium dioxide. *Dyes Pigm* 65(1):1–9. <https://doi.org/10.1016/j.dyepig.2004.06.006>
73. Mills A, Le Hunte S (1997) An overview of semiconductor photocatalysis. *J Photochem Photobiol, A* 108(1):1–35. [https://doi.org/10.1016/S1010-6030\(97\)00118-4](https://doi.org/10.1016/S1010-6030(97)00118-4)
74. Pirkanniemi K, Sillanpää M (2002) Heterogeneous water phase catalysis as an environmental application: a review. *Chemosphere* 48(10):1047–1060. [https://doi.org/10.1016/S0045-6535\(02\)00168-6](https://doi.org/10.1016/S0045-6535(02)00168-6)
75. Howe RF (1998) Recent developments in photocatalysis. *Dev Chem Eng Miner Process* 6(1–2):55–84. <https://doi.org/10.1002/apj.5500060105>

76. Aruna ST, Patil KC (1996) Synthesis and properties of nanosize titania. *J Mater Synth Process* 4:175–180
77. Tong H, Ouyang S, Bi Y, Umezawa N, Oshikiri M, Ye J (2012) Nano-photocatalytic materials: possibilities and challenges. *Adv Mater* 24(2):229–251. <https://doi.org/10.1002/adma.201102752>
78. Tsai MT, Chang YS, Liu YC (2017) Photocatalysis and luminescence properties of zinc stannate oxides. *Ceram Int* 43:S428–S434. <https://doi.org/10.1016/j.ceramint.2017.05.251>
79. Chen R, Bi J, Wu L, Li Z, Fu X (2009) Orthorhombic Bi_2GeO_5 nanobelts: synthesis, characterization, and photocatalytic properties. *Cryst Growth Des* 9(4):1775–1779. <https://doi.org/10.1021/cg800842f>
80. Foletto EL, Simões JM, Mazutti MA, Jahn SL, Muller EI, Pereira LSF, de Moraes Flores EM (2013) Application of Zn_2SnO_4 photocatalyst prepared by microwave-assisted hydrothermal route in the degradation of organic pollutant under sunlight. *Ceram Int* 39(4):4569–4574. <https://doi.org/10.1016/j.ceramint.2012.11.053>
81. Henglein A (1997) Nanoclusters of semiconductors and metals: Colloidal nano-particles of semiconductors and metals: Electronic structure and processes. *Ber Bunsenges Phys Chem* 101(11):1562–1572. <https://doi.org/10.1002/bbpc.19971011103>
82. Ye, M., Zhang, Q., Hu, Y., Ge, J., Lu, Z., He, L., Chen, Z. and Yin, Y., 2010. Magnetically recoverable core-shell nanocomposites with enhanced photocatalytic activity. *Chemistry—A European Journal*, 16(21), pp.6243–6250. <https://doi.org/10.1002/chem.200903516>.
83. Hariharan, C., 2006. Photocatalytic degradation of organic contaminants in water by ZnO nanoparticles: Revisited. *Applied Catalysis A: General*, 304, pp.55–61. <https://doi.org/10.1016/j.apcata.2006.02.020>.
84. Anpo, M., Shima, T., Kodama, S. and Kubokawa, Y., 1987. Photocatalytic hydrogenation of propyne with water on small-particle titania: size quantization effects and reaction intermediates. *Journal of Physical Chemistry*, 91(16), pp.4305–4310. <https://doi.org/10.1021/j100300a021>.
85. Kim DS, Kwak SY (2007) The hydrothermal synthesis of mesoporous TiO_2 with high crystallinity, thermal stability, large surface area, and enhanced photocatalytic activity. *Appl Catal A* 323:110–118. <https://doi.org/10.1016/j.apcata.2007.02.010>
86. Lin H, Huang CP, Li W, Ni C, Shah SI, Tseng YH (2006) Size dependency of nanocrystalline TiO_2 on its optical property and photocatalytic reactivity exemplified by 2-chlorophenol. *Appl Catal B* 68(1–2):1–11. <https://doi.org/10.1016/j.apcatb.2006.07.018>
87. Auyeung E, Morris W, Mondloch JE, Hupp JT, Farha OK, Mirkin CA (2015) Controlling structure and porosity in catalytic nanoparticle superlattices with DNA. *J Am Chem Soc* 137(4):1658–1662. <https://doi.org/10.1021/ja512116p>
88. Gheorghiu S, Coppens MO (2004) Optimal bimodal pore networks for heterogeneous catalysis. *AIChE J* 50(4):812–820. <https://doi.org/10.1002/aic.10076>
89. Ahmed S, Ahmad M, Swami BL, Ikram S (2016) A review on plants extract mediated synthesis of silver nanoparticles for antimicrobial applications: a green expertise. *J Adv Res* 7(1):17–28. <https://doi.org/10.1016/j.jare.2015.02.007>
90. An GH, Jo HG, Ahn HJ (2018) Platinum nanoparticles on nitrogen-doped carbon and nickel composites surfaces: a high electrical conductivity for methanol oxidation reaction. *J Alloy Compd* 763:250–256. <https://doi.org/10.1016/j.jallcom.2018.05.313>
91. Ting CC, Chao CH, Tsai CY, Cheng IK, Pan FM (2017) Electrocatalytic performance of Pt nanoparticles sputter-deposited on indium tin oxide toward methanol oxidation reaction: the particle size effect. *Appl Surf Sci* 416:365–370. <https://doi.org/10.1016/j.apsusc.2017.04.156>
92. Hou W, Dong X, Li Y, Zhang H, Xu L, Tian Y, Jiao A, Chen M (2019) Ultraviolet laser beam-assisted one-step synthesis of clean PtPd nanoarchitectures with excellent electrocatalytic properties for direct methanol fuel cells. *Mater Chem Phys* 221:409–418. <https://doi.org/10.1016/j.matchemphys.2018.09.073>
93. Tao W, Pan D, Gong Z, Peng X (2018) Nanoporous platinum electrode grown on anodic aluminum oxide membrane: Fabrication, characterization, electrocatalytic activity toward reactive oxygen and nitrogen species. *Anal Chim Acta* 1035:44–50. <https://doi.org/10.1016/j.aca.2018.06.076>
94. Chang HW, Tsai YC, Cheng CW, Lin CY, Wu PH (2013) Preparation of graphene-supported platinum nanoparticles in aqueous solution by femtosecond laser pulses for methanol oxidation. *J Power Sources* 239:164–168. <https://doi.org/10.1016/j.jpowsour.2013.03.119>
95. Bukka S, Badam R, Vedarajan R, Matsumi N (2019) Photo-generation of ultra-small Pt nanoparticles on carbon-titanium dioxide nanotube composites: A novel strategy for efficient ORR activity

- with low Pt content. *Int J Hydrogen Energy* 44(10):4745–4753. <https://doi.org/10.1016/j.ijhydene.2019.01.004>
96. Thakkar, K.N., Mhatre, S.S. and Parikh, R.Y., 2010. Biological synthesis of metallic nanoparticles. *Nanomedicine: nanotechnology, biology and medicine*, 6(2), pp.257–262. <https://doi.org/10.1016/j.nano.2009.07.002>.
97. Zheng F, Luk SY, Kwong TL, Yung KF (2016) Synthesis of hollow PtAg alloy nanospheres with excellent electrocatalytic performances towards methanol and formic acid oxidations. *RSC Adv* 6(50):44902–44907. <https://doi.org/10.1039/C6RA06398E>
98. Yahya N, Kamarudin SK, Karim NA, Masdar MS, Loh KS, Lim KL (2019) Durability and performance of direct glycerol fuel cell with palladium-aurum/vapor grown carbon nanofiber support. *Energy Convers Manage* 188:120–130. <https://doi.org/10.1016/j.enconman.2019.02.087>
99. Abdullah, M. and Kamarudin, S.K., 2017. Titanium dioxide nanotubes (TNT) in energy and environmental applications: An overview. *Renewable and Sustainable Energy Reviews*, 76, pp.212–225. <https://doi.org/10.1016/j.rser.2017.01.057>.
100. Fang WC, Chen FR, Tsai MC, Chou HY, Wu HC, Hsieh CK (2017) Electrochemical deposited high-crystallinity vertical platinum nanosheets onto the carbon nanotubes directly grown on carbon paper for methanol oxidation. *Surf Coat Technol* 320:584–589
101. Han L, Cui P, He H, Liu H, Peng Z, Yang J (2015) A seed-mediated approach to the morphology-controlled synthesis of bimetallic copper–platinum alloy nanoparticles with enhanced electrocatalytic performance for the methanol oxidation reaction. *J Power Sources* 286:488–494. <https://doi.org/10.1016/j.jpowsour.2015.04.003>
102. Karim NA, Kamarudin SK, Loh KS (2017) Performance of a novel non-platinum cathode catalyst for direct methanol fuel cells. *Energy Convers Manage* 145:293–307. <https://doi.org/10.1016/j.enconman.2017.05.003>
103. Liu D, Li L, You T (2017) Superior catalytic performances of platinum nanoparticles loaded nitrogen-doped graphene toward methanol oxidation and hydrogen evolution reaction. *J Colloid Interface Sci* 487:330–335. <https://doi.org/10.1016/j.jcis.2016.10.038>
104. Yu M, Wu X, Zhang J, Meng Y, Ma Y, Liu J, Li S (2017) Platinum nanoparticles-loaded holey reduced graphene oxide framework as freestanding counter electrodes of dye sensitized solar cells and methanol oxidation catalysts. *Electrochim Acta* 258:485–494. <https://doi.org/10.1016/j.electacta.2017.11.086>
105. Irvani S (2011) Green synthesis of metal nanoparticles using plants. *Green Chem* 13(10):2638–2650. <https://doi.org/10.1039/C1GC15386B>
106. Abdullah, N., Kamarudin, S.K., Shyuan, L.K. and Karim, N.A., 2019. Synthesis and optimization of PtRu/TiO₂-CNF anodic catalyst for direct methanol fuel cell. *International Journal of Hydrogen Energy*, 44(58), pp.30543–30552. <https://doi.org/10.1016/j.ijhydene.2018.05.042>.
107. Hemmati S, Rashtiani A, Zangeneh MM, Mohammadi P, Zangeneh A, Veisi H (2019) Green synthesis and characterization of silver nanoparticles using *Fritillaria* flower extract and their antibacterial activity against some human pathogens. *Polyhedron* 158:8–14. <https://doi.org/10.1016/j.poly.2018.10.049>
108. Sharma D, Kanchi S, Bisetty K (2019) Biogenic synthesis of nanoparticles: A review. *Arab J Chem* 12(8):3576–3600. <https://doi.org/10.1016/j.arabjc.2015.11.002>
109. Nadaroglu H, Gungor AA, Ince S, Babagil A (2017) Green synthesis and characterisation of platinum nanoparticles using quail egg yolk. *Spectrochim Acta Part A Mol Biomol Spectrosc* 172:43–47. <https://doi.org/10.1016/j.saa.2016.05.023>
110. Benelmekki, M., 2015. Designing hybrid nanoparticles (pp. 1–1). San Rafael: Morgan & Claypool Publishers. <https://doi.org/10.1088/978-1-6270-5469-0>
111. Mondal A, Mondal A, Adhikary B, Mukherjee DK (2017) Cobalt nanoparticles as reusable catalysts for reduction of 4-nitrophenol under mild conditions. *Bull Mater Sci* 40(2):321–328. <https://doi.org/10.1007/s12034-017-1367-3>
112. Kozakova Z, Kuritka I, Kazantseva NE, Babayan V, Pastorek M, Machovsky M, Bazant P, Saha P (2015) The formation mechanism of iron oxide nanoparticles within the microwave-assisted solvothermal synthesis and its correlation with the structural and magnetic properties. *Dalton Trans* 44(48):21099–21108. <https://doi.org/10.1039/C5DT03518J>
113. Lee KJ, Park SH, Govarthanan M, Hwang PH, Seo YS, Cho M, Lee WH, Lee JY, Kamalakannan S, Oh BT (2013) Synthesis of silver nanoparticles using cow milk and their antifungal

- activity against phytopathogens. *Mater Lett* 105:128–131. <https://doi.org/10.1016/j.matlet.2013.04.076>
114. Saha S, Pal A, Kundu S, Basu S, Pal T (2010) Photochemical green synthesis of calcium-alginate-stabilized Ag and Au nanoparticles and their catalytic application to 4-nitrophenol reduction. *Langmuir* 26(4):2885–2893. <https://doi.org/10.1021/la902950x>
 115. Newman JDS, Blanchard GJ (2006) Formation of gold nanoparticles using amine reducing agents. *Langmuir* 22(13):5882–5887. <https://doi.org/10.1021/la060045z>
 116. Vaseem M, Umar A, Hahn YB (2010) ZnO nanoparticles: growth, properties, and applications. *Metal oxide nanostructures and their applications* 5(1):10–20
 117. Malik, P., Shankar, R., Malik, V., Sharma, N. and Mukherjee, T.K., 2014. Green chemistry based benign routes for nanoparticle synthesis. *Journal of Nanoparticles*, 2014. <https://doi.org/10.1155/2014/302429>.
 118. Makarov, V.V., Love, A.J., Sinitynsya, O.V., Makarova, S.S., Yaminsky, I.V., Taliansky, M.E. and Kalinina, N.O., 2014. “Green” nanotechnologies: synthesis of metal nanoparticles using plants. *Acta Naturae (англоязычная версия)*, 6(1 (20)), pp.35–44.
 119. Lamri M, Bhattacharya T, Boukid F, Chentir I, Dib AL, Das D, Djenane D, Gagaoua M (2021) Nanotechnology as a processing and packaging tool to improve meat quality and safety. *Foods* 10(11):2633
 120. Mittal, A.K., Chisti, Y. and Banerjee, U.C., 2013. Synthesis of metallic nanoparticles using plant extracts. *Biotechnology advances*, 31(2), pp.346–356. <https://doi.org/10.1016/j.biotechadv.2013.01.003>.
 121. Elumalai K, Velmurugan S, Ravi S, Kathiravan V, Ashokkumar S (2015) Green synthesis of zinc oxide nanoparticles using *Moringa oleifera* leaf extract and evaluation of its antimicrobial activity. *Spectrochim Acta Part A Mol Biomol Spectrosc* 143:158–164. <https://doi.org/10.1016/j.saa.2015.02.011>
 122. Akhtar MS, Panwar J, Yun YS (2013) Biogenic synthesis of metallic nanoparticles by plant extracts. *ACS Sustainable Chemistry & Engineering* 1(6):591–602. <https://doi.org/10.1021/sc300118u>
 123. Ruddaraju LK, Pammi SVN, sankar Guntuku, G., Padavala, V.S. and Kolapalli, V.R.M. (2020) A review on anti-bacterials to combat resistance: From ancient era of plants and metals to present and future perspectives of green nano technological combinations. *Asian J Pharm Sci* 15(1):42–59. <https://doi.org/10.1016/j.ajps.2019.03.002>
 124. Naveed Ul Haq, A., Nadhman, A., Ullah, I., Mustafa, G., Yasinzai, M. and Khan, I., 2017. Synthesis approaches of zinc oxide nanoparticles: the dilemma of ecotoxicity. *Journal of Nanomaterials*, 2017. <https://doi.org/10.1155/2017/8510342>.
 125. Naikoo GA, Mustaqeem M, Hassan IU, Awan T, Arshad F, Salim H, Qurashi A (2021) Bioinspired and green synthesis of nanoparticles from plant extracts with antiviral and antimicrobial properties: A critical review. *J Saudi Chem Soc* 25(9):101304
 126. Kumar, S., Terashima, C., Fujishima, A., Krishnan, V. and Pitchaimuthu, S., 2019. Photocatalytic degradation of organic pollutants in water using graphene oxide composite. In *A new generation material graphene: applications in water technology* (pp. 413–438). Springer, Cham. https://doi.org/10.1007/978-3-319-75484-0_17.
 127. Lee KM, Lai CW, Ngai KS, Juan JC (2016) Recent developments of zinc oxide based photocatalyst in water treatment technology: a review. *Water Res* 88:428–448. <https://doi.org/10.1016/j.watres.2015.09.045>
 128. Wu W, Zhang S, Ren F, Xiao X, Zhou J, Jiang C (2011) Controlled synthesis of magnetic iron oxides@SnO₂ quasi-hollow core-shell heterostructures: formation mechanism, and enhanced photocatalytic activity. *Nanoscale* 3(11):4676–4684. <https://doi.org/10.1039/C1NR10728C>
 129. Naushad M, Mittal A, Rathore M, Gupta V (2015) Ion-exchange kinetic studies for Cd (II), Co (II), Cu (II), and Pb (II) metal ions over a composite cation exchanger. *Desalination Water Treatment* 54:2883–2890. <https://doi.org/10.1080/19443994.2014.904823>
 130. Lin, Z., Ye, M. and Wang, M. eds., 2018. Multifunctional photocatalytic materials for energy. Woodhead Publishing.
 131. Fox MA, Dulay MT (1993) Heterogeneous photocatalysis. *Chem Rev* 93(1):341–357
 132. Herrmann, J.M., 2005. Heterogeneous photocatalysis: state of the art and present applications In honor of Pr. RL Burwell Jr.(1912–2003), Former Head of Ipatieff Laboratories, Northwestern University, Evanston (Ill). *Topics in catalysis*, 34(1), pp.49–65. <https://doi.org/10.1007/s11244-005-3788-2>.

133. Herrmann JM (1999) Heterogeneous photocatalysis: fundamentals and applications to the removal of various types of aqueous pollutants. *Catal Today* 53(1):115–129. [https://doi.org/10.1016/S0920-5861\(99\)00107-8](https://doi.org/10.1016/S0920-5861(99)00107-8)
134. Reza KM, Kurny ASW, Gulshan F (2017) Parameters affecting the photocatalytic degradation of dyes using TiO_2 : a review. *Appl Water Sci* 7(4):1569–1578. <https://doi.org/10.1007/s13201-015-0367>
135. Akpan UG, Hameed BH (2009) Parameters affecting the photocatalytic degradation of dyes using TiO_2 -based photocatalysts: a review. *J Hazard Mater* 170(2–3):520–529. <https://doi.org/10.1016/j.jhazmat.2009.05.039>
136. Davis RJ, Gainer JL, O'Neal G, Wu IW (1994) Photocatalytic decolorization of wastewater dyes. *Water Environ Res* 66(1):50–53
137. Kormann C, Bahnemann DW, Hoffmann MR (1988) Photocatalytic production of hydrogen peroxides and organic peroxides in aqueous suspensions of titanium dioxide, zinc oxide, and desert sand. *Environ Sci Technol* 22(7):798–806. <https://doi.org/10.1021/es00172a009>
138. Zhu J, Deng Z, Chen F, Zhang J, Chen H, Anpo M, Huang J, Zhang L (2006) Hydrothermal doping method for preparation of Cr^{3+} - TiO_2 photocatalysts with concentration gradient distribution of Cr^{3+} . *Appl Catal B* 62(3–4):329–335. <https://doi.org/10.1016/j.apcatb.2005.08.013>
139. Ameen S, Seo HK, Akhtar MS, Shin HS (2012) Novel graphene/polyaniline nanocomposites and its photocatalytic activity toward the degradation of rose Bengal dye. *Chem Eng J* 210:220–228. <https://doi.org/10.1016/j.cej.2012.08.035>
140. Mamba G, Mamo MA, Mbianda XY, Mishra AK (2014) Nd, N, S- TiO_2 decorated on reduced graphene oxide for a visible light active photocatalyst for dye degradation: Comparison to its MWCNT/Nd, N, S- TiO_2 analogue. *Ind Eng Chem Res* 53(37):14329–14338. <https://doi.org/10.1021/ie502610y>
141. Hashimoto K, Irie H, Fujishima A (2005) TiO_2 photocatalysis: a historical overview and future prospects. *Jpn J Appl Phys* 44(12R):8269. <https://doi.org/10.1143/JJAP.44.8269>
142. Mills A, Davies RH, Worsley D (1993) Water purification by semiconductor photocatalysis. *Chem Soc Rev* 22(6):417–425. <https://doi.org/10.1039/CS9932200417>
143. Asahi, R.Y.O.J.I., Morikawa, T.A.K.E.S.H.I., Ohwaki, T., Aoki, K. and Taga, Y., 2001. Visible-light photocatalysis in nitrogen-doped titanium oxides. *science*, 293(5528), pp.269–271. <https://doi.org/10.1126/science.1061051>.
144. Rajeshwar K, Osugi ME, Chanmanee W, Chenthamarakshan CR, Zanon MVB, Kajitvichyanukul P, Krishnan-Ayer R (2008) Heterogeneous photocatalytic treatment of organic dyes in air and aqueous media. *J Photochem Photobiol, C* 9(4):171–192. <https://doi.org/10.1016/j.jphotochemrev.2008.09.001>
145. Maeda K (2011) Photocatalytic water splitting using semiconductor particles: history and recent developments. *J Photochem Photobiol, C* 12(4):237–268. <https://doi.org/10.1016/j.jphotochemrev.2011.07.001>
146. Abe R (2010) Recent progress on photocatalytic and photoelectrochemical water splitting under visible light irradiation. *J Photochem Photobiol, C* 11(4):179–209. <https://doi.org/10.1016/j.jphotochemrev.2011.02.003>
147. Ola O, Maroto-Valer MM (2015) Review of material design and reactor engineering on TiO_2 photocatalysis for CO_2 reduction. *J Photochem Photobiol, C* 24:16–42. <https://doi.org/10.1016/j.jphotochemrev.2015.06.001>
148. Gupta, S.M. and Tripathi, M., 2011. A review of TiO_2 nanoparticles. *chinese science bulletin*, 56(16), pp.1639–1657. <https://doi.org/10.1007/s1143401144761>.
149. Bahnemann DW, Kormann C, Hoffmann MR (1987) Preparation and characterization of quantum size zinc oxide: a detailed spectroscopic study. *J Phys Chem* 91(14):3789–3798. <https://doi.org/10.1021/j100298a015>
150. Tamirat AG, Rick J, Dubale AA, Su WN, Hwang BJ (2016) Using hematite for photoelectrochemical water splitting: a review of current progress and challenges. *Nanoscale Horizons* 1(4):243–267. <https://doi.org/10.1039/C5NH00098J>
151. Neamen, D.A., 2003. *Semiconductor physics and devices: basic principles*. McGraw-hill.
152. Zhang Q, Gangadharan DT, Liu Y, Xu Z, Chaker M, Ma D (2017) Recent advancements in plasmon-enhanced visible light-driven water splitting. *Journal of Materiomics* 3(1):33–50. <https://doi.org/10.1016/j.jmat.2016.11.005>

153. Malwal D, Gopinath P (2016) Fabrication and applications of ceramic nanofibers in water remediation: a review. *Crit Rev Environ Sci Technol* 46(5):500–534. <https://doi.org/10.1080/10643389.2015.1109913>
154. Zhou L, Zhang C, McClain MJ, Manjavacas A, Krauter CM, Tian S, Berg F, Everitt HO, Carter EA, Nordlander P, Halas NJ (2016) Aluminum nanocrystals as a plasmonic photocatalyst for hydrogen dissociation. *Nano Lett* 16(2):1478–1484. <https://doi.org/10.1021/acs.nanolett.5b05149>
155. Liang X, Wang P, Li M, Zhang Q, Wang Z, Dai Y, Zhang X, Liu Y, Whangbo MH, Huang B (2018) Adsorption of gaseous ethylene via induced polarization on plasmonic photocatalyst Ag/AgCl/TiO₂ and subsequent photodegradation. *Appl Catal B* 220:356–361. <https://doi.org/10.1016/j.apcatb.2017.07.075>
156. Dong F, Xiong T, Sun Y, Zhao Z, Zhou Y, Feng X, Wu Z (2014) A semimetal bismuth element as a direct plasmonic photocatalyst. *Chem Commun* 50(72):10386–10389. <https://doi.org/10.1039/C4CC02724H>
157. Yang, Y., Guo, W., Guo, Y., Zhao, Y., Yuan, X. and Guo, Y., 2014. Fabrication of Z-scheme plasmonic photocatalyst Ag@AgBr/g-C₃N₄ with enhanced visible-light photocatalytic activity. *Journal of hazardous materials*, 271, pp.150–159. <https://doi.org/10.1016/j.jhazmat.2014.02.023>.
158. Wang, C. and Astruc, D., 2014. Nanogold plasmonic photocatalysis for organic synthesis and clean energy conversion. *Chemical Society Reviews*, 43(20), pp.7188–7216. <https://doi.org/10.1039/C4CS00145A>.
159. Thomann I, Pinaud BA, Chen Z, Clemens BM, Jaramillo TF, Brongersma ML (2011) Plasmon enhanced solar-to-fuel energy conversion. *Nano Lett* 11(8):3440–3446. <https://doi.org/10.1021/nl201908s>
160. Morgan BJ, Watson GW (2010) Intrinsic n-type defect formation in TiO₂: a comparison of rutile and anatase from GGA+ U calculations. *The Journal of Physical Chemistry C* 114(5):2321–2328. <https://doi.org/10.1021/jp9088047>
161. Zhu Z (2017) An overview of carbon nanotubes and graphene for biosensing applications. *Nano-micro letters* 9(3):1–24. <https://doi.org/10.1007/s40820-017-0128-6>
162. Hebbar RS, Isloor AM, Asiri AM (2017) Carbon nanotube-and graphene-based advanced membrane materials for desalination. *Environ Chem Lett* 15(4):643–671. <https://doi.org/10.1007/s10311-017-0653-z>
163. Williams, G., Seger, B. and Kamat, P.V., 2008. TiO₂-graphene nanocomposites. UV-assisted photocatalytic reduction of graphene oxide. *ACS nano*, 2(7), pp.1487–1491. <https://doi.org/10.1021/nm800251f>.
164. Suárez-Iglesias O, Collado S, Oulego P, Díaz M (2017) Graphene-family nanomaterials in wastewater treatment plants. *Chem Eng J* 313:121–135. <https://doi.org/10.1016/j.cej.2016.12.022>
165. El-Nemr, M.A., Aigbe, U.O., Hassaan, M.A., Ukhurebor, K.E., Ragab, S., Onyancha, R.B., Osibote, O.A. and El Nemr, A., 2022. The use of biochar-NH₂ produced from watermelon peels as a natural adsorbent for the removal of Cu (II) ion from water. *Biomass Conversion and Biorefinery*, pp.1–17.
166. Li X, Yu J, Wageh S, Al-Ghamdi AA, Xie J (2016) Graphene in photocatalysis: a review. *Small* 12(48):6640–6696. <https://doi.org/10.1002/sml.201600382>
167. Qin J, Yang C, Cao M, Zhang X, Rajendran S, Limpanart S, Ma M, Liu R (2017) Two-dimensional porous sheet-like carbon-doped ZnO/g-C₃N₄ nanocomposite with high visible-light photocatalytic performance. *Mater Lett* 189:156–159. <https://doi.org/10.1016/j.matlet.2016.12.007>
168. Gnanasekaran S, Saravanan N, Ilangkumaran M (2016) Influence of injection timing on performance, emission and combustion characteristics of a DI diesel engine running on fish oil biodiesel. *Energy* 116:1218–1229. <https://doi.org/10.1016/j.energy.2016.10.039>
169. Romero-Sáez M, Jaramillo LY, Saravanan R, Benito N, Pabón E, Mosquera E, Gracia F (2017) Notable photocatalytic activity of TiO₂ sub 2-polyethylene nanocomposites for visible light degradation of organic pollutants. *Express Polym Lett* 11(11):899–909. <https://doi.org/10.3144/expresspolymlett.2017.86>
170. Saravanan R, Manoj D, Qin J, Naushad M, Gracia F, Lee AF, Khan MM, Gracia-Pinilla MA (2018) Mechanochemical synthesis of Ag/TiO₂ for photocatalytic methyl orange degradation and hydrogen production. *Process Saf Environ Prot* 120:339–347. <https://doi.org/10.1016/j.psep.2018.09.015>
171. Mandal D, Bolander ME, Mukhopadhyay D, Sarkar G, Mukherjee P (2006) The use of microorganisms for the formation of metal nanoparticles and their application. *Appl Microbiol Biotechnol* 69(5):485–492. <https://doi.org/10.1007/s00253-005-0179-3>
172. Narayanan, K.B. and Sakhivel, N., 2011. Synthesis and characterization of nano-gold composite using *Cylindroclostridium floridanum* and its heterogeneous catalysis in the degradation of

- 4-nitrophenol. *Journal of hazardous materials*, 189(1–2), pp.519–525.<https://doi.org/10.1016/j.jhazmat.2011.02.069>.
173. Khan R, Fulekar MH (2016) Biosynthesis of titanium dioxide nanoparticles using *Bacillus amyloliquefaciens* culture and enhancement of its photocatalytic activity for the degradation of a sulfonated textile dye Reactive Red 31. *J Colloid Interface Sci* 475:184–191. <https://doi.org/10.1016/j.jcis.2016.05.001>
 174. Dhandapani P, Maruthamuthu S, Rajagopal G (2012) Bio-mediated synthesis of TiO₂ nanoparticles and its photocatalytic effect on aquatic biofilm. *J Photochem Photobiol, B* 110:43–49. <https://doi.org/10.1016/j.jphotobiol.2012.03.003>
 175. Tripathi, R.M., Bhadwal, A.S., Gupta, R.K., Singh, P., Shrivastav, A. and Shrivastav, B.R., 2014. ZnO nanoflowers: novel biogenic synthesis and enhanced photocatalytic activity. *Journal of Photochemistry and Photobiology B: Biology*, 141, pp.288–295.<https://doi.org/10.1016/j.jphotobiol.2014.10.001>.
 176. Jain N, Bhargava A, Panwar J (2014) Enhanced photocatalytic degradation of methylene blue using biologically synthesized “protein-capped” ZnO nanoparticles. *Chem Eng J* 243:549–555. <https://doi.org/10.1016/j.cej.2013.11.085>
 177. Bhadwal AS, Tripathi RM, Gupta RK, Kumar N, Singh RP, Shrivastav A (2014) Biogenic synthesis and photocatalytic activity of CdS nanoparticles. *RSC Adv* 4(19):9484–9490. <https://doi.org/10.1039/c3ra46221h>
 178. Rao MD, Gautam P (2016) Synthesis and characterization of ZnO nanoflowers using *Chlamydomonas reinhardtii*: A green approach. *Environ Prog Sustainable Energy* 35(4):1020–1026. <https://doi.org/10.1002/ep.12315>
 179. Pantidos N, Horsfall LE (2014) Biological synthesis of metallic nanoparticles by bacteria, fungi and plants. *Journal of Nanomedicine & Nanotechnology* 5(5):1. <https://doi.org/10.4172/2157-7439.1000233>
 180. Ramesh, M., Anbuvannan, M. and Viruthagiri, G.J.S.A.P.A.M., 2015. Green synthesis of ZnO nanoparticles using *Solanum nigrum* leaf extract and their antibacterial activity. *Spectrochimica Acta Part A: Molecular and Biomolecular Spectroscopy*, 136, pp.864–870.<https://doi.org/10.1016/j.saa.2014.09.105>.
 181. Shankar, S.S., Rai, A., Ankamwar, B., Singh, A., Ahmad, A. and Sastry, M., 2004. Biological synthesis of triangular gold nanoprisms. *Nature materials*, 3(7), pp.482–488.<https://doi.org/10.1038/nmat1152>.
 182. Nagajyothi PC, Cha SJ, Yang IJ, Sreekanth TVM, Kim KJ, Shin HM (2015) Antioxidant and anti-inflammatory activities of zinc oxide nanoparticles synthesized using *Polygala tenuifolia* root extract. *J Photochem Photobiol, B* 146:10–17. <https://doi.org/10.1016/j.jphotobiol.2015.02.008>
 183. Elango G, Kumaran SM, Kumar SS, Muthuraja S, Roopan SM (2015) Green synthesis of SnO₂ nanoparticles and its photocatalytic activity of phenolsulfonphthalein dye. *Spectrochim Acta Part A Mol Biomol Spectrosc* 145:176–180. <https://doi.org/10.1016/j.saa.2015.03.033>
 184. Haritha E, Roopan SM, Madhavi G, Elango G, Al-Dhabi NA, Arasu MV (2016) Green chemical approach towards the synthesis of SnO₂ NPs in argument with photocatalytic degradation of diazo dye and its kinetic studies. *J Photochem Photobiol, B* 162:441–447. <https://doi.org/10.1016/j.jphotobiol.2016.07.010>
 185. Surendra TV, Roopan SM (2016) Photocatalytic and antibacterial properties of phytosynthesized CeO₂ NPs using *Moringa oleifera* peel extract. *J Photochem Photobiol, B* 161:122–128. <https://doi.org/10.1016/j.jphotobiol.2016.05.019>
 186. Kumar B, Smita K, Cumbal L, Debut A, Galeas S, Guerrero VH (2016) Phytosynthesis and photocatalytic activity of magnetite (Fe₃O₄) nanoparticles using the Andean blackberry leaf. *Mater Chem Phys* 179:310–315. <https://doi.org/10.1016/j.matchemphys.2016.05.045>
 187. Bishnoi, S., Kumar, A. and Selvaraj, R., 2018. Facile synthesis of magnetic iron oxide nanoparticles using inedible *Cynometra ramiflora* fruit extract waste and their photocatalytic degradation of methylene blue dye. *Materials Research Bulletin*, 97, pp.121–127.<https://doi.org/10.1016/j.materresbull.2017.08.040>.
 188. Naik, G.K., Mishra, P.M. and Parida, K., 2013. Green synthesis of Au/TiO₂ for effective dye degradation in aqueous system. *Chemical Engineering Journal*, 229, pp.492–497.<https://doi.org/10.1016/j.cej.2013.06.053>.
 189. Rostami-Vartooni A, Nasrollahzadeh M, Salavati-Niasari M, Atarod M (2016) Photocatalytic degradation of azo dyes by titanium dioxide supported silver nanoparticles prepared by a green method

- using *Carpobrotus acinaciformis* extract. *J Alloy Compd* 689:15–20. <https://doi.org/10.1016/j.jallcom.2016.07.253>
190. Sankar R, Rizwana K, Shivashangari KS, Ravikumar V (2015) Ultra-rapid photocatalytic activity of *Azadirachta indica* engineered colloidal titanium dioxide nanoparticles. *Appl Nanosci* 5(6):731–736. <https://doi.org/10.1007/s13204-014-0369-3>
191. Goutam, S.P., Saxena, G., Singh, V., Yadav, A.K., Bharagava, R.N. and Thapa, K.B., 2018. Green synthesis of TiO₂ nanoparticles using leaf extract of *Jatropha curcas* L. for photocatalytic degradation of tannery wastewater. *Chemical Engineering Journal*, 336, pp.386–396. <https://doi.org/10.1016/j.cej.2017.12.029>.
192. Karnan T, Selvakumar SAS (2016) Biosynthesis of ZnO nanoparticles using rambutan (*Nephelium lappaceum* L.) peel extract and their photocatalytic activity on methyl orange dye. *J Mol Struct* 1125:358–365. <https://doi.org/10.1016/j.molstruc.2016.07.029>
193. Nava OJ, Luque PA, Gómez-Gutiérrez CM, Vilchis-Nestor AR, Castro-Beltrán A, Mota-González ML, Olivás A (2017) Influence of *Camellia sinensis* extract on Zinc Oxide nanoparticle green synthesis. *J Mol Struct* 1134:121–125. <https://doi.org/10.1016/j.molstruc.2016.12.069>
194. Sharma SC (2016) ZnO nano-flowers from *Carica papaya* milk: degradation of Alizarin Red-S dye and antibacterial activity against *Pseudomonas aeruginosa* and *Staphylococcus aureus*. *Optik* 127(16):6498–6512. <https://doi.org/10.1016/j.ijleo.2016.04.036>
195. Fatimah I, Pradita RY, Nurfalinda A (2016) Plant extract mediated of ZnO nanoparticles by using ethanol extract of *Mimosa pudica* leaves and coffee powder. *Procedia engineering* 148:43–48. <https://doi.org/10.1016/j.proeng.2016.06.483>
196. Fowsiya J, Madhumitha G, Al-Dhabi NA, Arasu MV (2016) Photocatalytic degradation of Congo red using *Carissa edulis* extract capped zinc oxide nanoparticles. *J Photochem Photobiol, B* 162:395–401. <https://doi.org/10.1016/j.jphotobiol.2016.07.011>
197. Raja A, Ashokkumar S, Marthandan RP, Jayachandiran J, Khatiwada CP, Kaviyarasu K, Raman RG, Swaminathan M (2018) Eco-friendly preparation of zinc oxide nanoparticles using *Tabernaemontana divaricata* and its photocatalytic and antimicrobial activity. *J Photochem Photobiol, B* 181:53–58. <https://doi.org/10.1016/j.jphotobiol.2018.02.011>
198. Archana, B., Manjunath, K., Nagaraju, G., Sekhar, K.C. and Kottam, N., 2017. Enhanced photocatalytic hydrogen generation and photostability of ZnO nanoparticles obtained via green synthesis. *International Journal of Hydrogen Energy*, 42(8), pp.5125–5131. <https://doi.org/10.1016/j.ijhydene.2016.2016>.
199. Vidya C, Prabha MNC, Raj MALA (2016) Green mediated synthesis of zinc oxide nanoparticles for the photocatalytic degradation of Rose Bengal dye. *Environ Nanotechnology, Monitoring Management* 6:134–138. <https://doi.org/10.1016/j.enmm.2016.09.004>
200. Mirzadeh S, Darezereshki E, Bakhtiari F, Fazaelpoor MH, Hosseini MR (2013) Characterization of zinc sulfide (ZnS) nanoparticles Biosynthesized by *Fusarium oxysporum*. *Mater Sci Semicond Process* 16:374–378
201. Ahmad A, Mukherjee P, Mandal D, Senapati S, Khan MI, Kumar R, Sastry M (2002) Enzyme mediated extracellular synthesis of CdS nanoparticles by the fungus, *Fusarium oxysporum*. *J Am Chem Soc* 124:12108–12109
202. Tang WZ, Huang CP (1995) Inhibitory effect of thioacetamide on CdS dissolution during photocatalytic oxidation of 2, 4-dichlorophenol. *Chemosphere* 30:1385–1399
203. Senapati US, Jha DK, Sarkar D (2015) Structural, optical, thermal and electrical properties of fungus guided biosynthesized zinc sulphide nanoparticles. *Research Journal of Chemical Sciences* ISSN 2231:606X
204. Ayodhya D, Veerabhadram G (2017) One-pot green synthesis, characterization, photocatalytic, sensing and antimicrobial studies of *Calotropis gigantea* leaf extract capped CdS NPs. *Mater Sci Eng B* 225:33–44
205. Samanta D, Chanu TI, Chatterjee S (2017) Citrus limetta juice as capping agent in hydrothermal synthesis of ZnS nanosphere for photocatalytic activity. *Mater Res Bull* 88:85–90
206. Chen J, Hu B, Zhi J (2016) Optical and photocatalytic properties of *Corymbia citriodora* leaf extract synthesized ZnS nanoparticles. *Phys E Low-dimens Syst Nanostruct* 79:103–106
207. Rajabi HR, Sajadiasl F, Karimi H, Alvand ZM (2020) Green synthesis of Zinc Sulfide nanophotocatalysts using aqueous extract of *Ficus Johannis* plant for efficient photodegradation of some pollutants. *J Market Res* 9(6):15638–15647

208. Ullah A, Rasheed S, Ali I, Ullah N (2021) Plant Mediated Synthesis of CdS Nanoparticles, their characterization and application for photocatalytic degradation of toxic organic dye. *Chemical Review and Letters* 4:98–107
209. Wei Y, Fang Z, Zheng L, Tan L, Tsang EP (2016) Green synthesis of Fe nanoparticles using *Citrus maxima* peels aqueous extracts. *Mater Lett* 185:384–386
210. Truskewycz A, Shukla R, Ball AS (2016) Iron nanoparticles synthesized using green tea extracts for the Fenton-like degradation of concentrated dye mixtures at elevated temperatures. *J Environ Chem Eng* 4:4409–4417
211. Bibi I, Nazara N, Atab S, Sultan M, Ali A, Abbas A, Jilani K, Kamal S, Sarim FMM, Khang I, Jalalh F, Iqbal M (2019) Green synthesis of iron oxide nanoparticles using pomegranate seeds extract and photocatalytic activity evaluation for the degradation of textile dye. *J Mater Res Technol.* <https://doi.org/10.1016/j.jmrt.2019.10.006>
212. Bishnoi S, Kumar A, Selvaraj R (2017) Facile synthesis of magnetic iron oxide nanoparticles using inedible *Cynometra ramiflora* fruit extract waste and their photocatalytic degradation of methylene blue dye. *Mater Res Bull.* <https://doi.org/10.1016/j.materresbull.2017.08.040>
213. Arularasu MV, Devakumar J, Rajendran TV (2018) An innovative approach for green synthesis of iron oxide nanoparticles: Characterization and its photocatalytic activity. *Polyhedron.* <https://doi.org/10.1016/j.poly.2018.09.036>
214. Sanchez GR, Castilla CL, Gomez NB, Garcia A, Marcos R, Carmona ER (2016) Leaf extract from the endemic plant *Peumus boldus* as an effective bioproduct for the green synthesis of silver nanoparticles. *Mater Lett* 183:255–260
215. Muthulakshmi L, Rajini N, Nellaiah H, Kathiresan T (2017) Rajulu AV, Jawaid M, Preparation and properties of cellulose nanocomposite films with in situ generated copper nanoparticles using *Terminalia catappa* leaf extract. *Int J Biol Macromol* 95:1064–1071
216. Stan M, Popa A, Toloman D, Dehelean A, Lung I, Katona G (2015) Enhanced photocatalytic degradation properties of zinc oxide nanoparticles synthesized by using plant extracts. *Mater Sci Semicond Proces* 39:23–29
217. Beheshtkhou N, Kouhbanani MAJ, Savardashtaki A et al (2018) Green synthesis of iron oxide nanoparticles by aqueous leaf extract of *Daphne mezereum* as a novel dye removing material. *Appl Phys A* 124:363. <https://doi.org/10.1007/s00339-018-1782-3>
218. Muthukumar H, Chandrasekaran NI, Mohammed SN (2017) Pichiah S, Manickam M, Iron oxide nano-material: physicochemical traits and in vitro antibacterial propensity against multidrug resistant bacteria. *J Ind Eng Chem* 45:121–130
219. Bishnoi S, Kumar A, Selvaraj R (2018) Facile synthesis of magnetic iron oxide nanoparticles using inedible *Cynometra ramiflora* fruit extract waste and their photocatalytic degradation of methylene blue dye. *Mater Res Bull* 97:121–127
220. Bai H, Zhang Z, Guo Y, Jia W (2009) Biological synthesis of size-controlled cadmium sulfide nanoparticles using immobilized *Rhodobacter sphaeroides*. *Nanoscale Res Lett* 4:717
221. Bai HJ, Zhang ZM, Guo Y, Yang GE (2009) Biosynthesis of cadmium sulfide nanoparticles by photosynthetic bacteria *Rhodospseudomonas palustris*. *Colloids Surf B Biointerfaces* 70:142–146
222. A. Shivashankarappa, K.R. Sanjay, *Escherichia coli*-based synthesis of cadmium sulfide nanoparticles, characterization, antimicrobial and cytotoxicity studies, *Braz. J. Microbiol.* (2020) 1–10.
223. Fatima B, Siddiqui SI, Rajor HK, Malik MA, Narasimharao K, Ahmad R, Vikrant K, Kim T, Kim K-H (2023) Photocatalytic removal of organic dye using green synthesized zinc oxide coupled cadmium tungstate nanocomposite under natural solar light irradiation. *Environ Res* 216:114534
224. Surendra TV, Roopan SM (2016) Photocatalytic and antibacterial properties of photosynthesized CeO₂ NPs using *Moringa oleifera* peel extract. *J Photochem Photobiol B Biol* 161:122–1288
225. Miri A, Sarani M (2018) Biosynthesis, characterization and cytotoxic activity of CeO₂ nanoparticles. *Ceram Int* 44(11):12642–12647
226. Elahi B, Mirzaee M, Darroudi M, Oskuee RK, Sadri K, Amiri MS (2019) Preparation of cerium oxide nanoparticles in *Salvia macrosiphon* boiss seeds extract and investigation of their photocatalytic activities. *Ceram Int* 45(4):4790–4797
227. Helmy ET, El Nemr A, Mousa M, Arafa E, Eldafrawy S (2018) Photocatalytic degradation of organic dyes pollutants in the industrial textile wastewater by using synthesized TiO₂, C-doped TiO₂, S-doped TiO₂ and C, S co-doped TiO₂ nanoparticles. *J Water Environ Nanotechnol* 3(2):116–127

228. Raliya R, Biswas P, Tarafdar JC (2015) TiO₂ nanoparticle biosynthesis and its physiological effect on mung bean (*Vigna radiata* L.). *Biotechnol Rep* 5:22–26
229. Amirante R, Demastro G, Distaso E, Hassaan MA, Mormando A, Pantaleo AM, Tamburrano P, Tedone L, Clodoveo ML (2018) Effects of ultrasound and green synthesis ZnO nanoparticles on biogas production from Olive Pomace. *Energy Procedia* 148:940–947
230. Nethravathi PC, Shruthi GS, Suresh D, Nagabhushana H, Sharma SC (2015) *Garcinia xanthochymus* mediated green synthesis of ZnO nanoparticles: photoluminescence, photocatalytic and antioxidant activity studies. *Ceram Int* 41(7):8680–8687
231. Khan ZU, Sadiq HM, Shah NS, Khan AU, Muhammad N, Hassan SU, Tahir K, Khan FU, Imran M, Ahmad N, Ullah F (2019) Greener synthesis of zinc oxide nanoparticles using *Trianthema portulacastrum* extract and evaluation of its photocatalytic and biological applications. *J Photochem Photobiol B Biol* 192:147–157
232. Stan M, Lung I, Soran ML, Leostean C, Popa A, Stefan M, Lazar MD, Opris O, Silipas TD, orav AS, (2017) Removal of antibiotics from aqueous solutions by green synthesized magnetite nanoparticles with selected agro-waste extracts. *Process Saf Environ Prot* 107:357–372
233. Sethy NK, Arif Z, Mishra PK, Kumar P (2020) Green synthesis of TiO₂ nanoparticles from *Syzygium cumini* extract for photo-catalytic removal of lead (Pb) in explosive industrial wastewater. *Green Processing and Synthesis* 9(1):171–181
234. Lung I, Stan M, Opris O, Soran ML, Senila M, Stefan M (2018) Removal of lead (II), cadmium (II), and arsenic (III) from aqueous solution using magnetite nanoparticles prepared by green synthesis with Box-Behnken design. *Anal Lett* 51(16):2519–2531
235. Mahmoud AED, Al-Qahtani KM, Alflajj SO, Al-Qahtani SF, Alsamhan FA (2021) Green copper oxide nanoparticles for lead, nickel, and cadmium removal from contaminated water. *Sci Rep* 11(1):1–13
236. Ravikumar KVG, Sudakaran SV, Ravichandran K, Pulimi M, Natarajan C, Mukherjee A (2019) Green synthesis of NiFe nano particles using *Punica granatum* peel extract for tetracycline removal. *J Clean Prod* 210:767–776
237. Debnath B, Majumdar M, Bhowmik M, Bhowmik KL, Debnath A, Roy DN (2020) The effective adsorption of tetracycline onto zirconia nanoparticles synthesized by novel microbial green technology. *J Environ Manag* 261:110235
238. Pakzad K, Alinezhad H, Nasrollahzadeh M (2020) *Euphorbia polygonifolia* extract assisted biosynthesis of Fe₃O₄@CuO nanoparticles: applications in the removal of metronidazole, ciprofloxacin and cephalixin antibiotics from aqueous solutions under UV irradiation. *Appl Organomet Chem* 34(11):e5910
239. Khan SA, Shahid S, Shahid B, Fatima U, Abbasi SA (2020) Green synthesis of MnO nanoparticles using *Abutilon indicum* leaf extract for biological, photocatalytic, and adsorption activities. *Biomolecules* 10(5):785
240. Mahanty S, Chatterjee S, Ghosh S, Tudu P, Gaine T, Bakshi M, Chaudhuri P (2020) Synergistic approach towards the sustainable management of heavy metals in wastewater using mycosynthesized iron oxide nanoparticles: biofabrication, adsorptive dynamics and chemometric modeling study. *J Water Process Eng* 37:101426
241. Zimmerle, D., Duggan, G., Vaughn, T., Bell, C., Lute, C., Bennett, K., Kimura, Y., Cardoso-Saldaña, F.J. and Allen, D.T., 2022. Modeling air emissions from complex facilities at detailed temporal and spatial resolution: The Methane Emission Estimation Tool (MEET). *Science of The Total Environment*, p.153653. <https://doi.org/10.1016/j.scitotenv.2022.153653>.
242. Rodriguez SM, Gálvez JB, Rubio MM, Ibáñez PF, Padilla DA, Pereira MC, Mendes JF, De Oliveira JC (2004) Engineering of solar photocatalytic collectors. *Sol Energy* 77(5):513–524. <https://doi.org/10.1016/j.solener.2004.03.020>
243. Alfano OM, Bahnemann D, Cassano AE, Dillert R, Goslich R (2000) Photocatalysis in water environments using artificial and solar light. *Catal Today* 58(2–3):199–230. [https://doi.org/10.1016/S0920-5861\(00\)00252-2](https://doi.org/10.1016/S0920-5861(00)00252-2)
244. Monllor-Satoca D, Gómez R, González-Hidalgo M, Salvador P (2007) The “Direct–Indirect” model: An alternative kinetic approach in heterogeneous photocatalysis based on the degree of interaction of dissolved pollutant species with the semiconductor surface. *Catal Today* 129(1–2):247–255. <https://doi.org/10.1016/j.cattod.2007.08.002>
245. Carp O, Huisman CL, Reller A (2004) Photoinduced reactivity of titanium dioxide. *Prog Solid State Chem* 32(1–2):33–177. <https://doi.org/10.1016/j.progsolidstchem.2004.08.001>

246. Ajona JI, Vidal A (2000) The use of CPC collectors for detoxification of contaminated water: Design, construction and preliminary results. *Sol Energy* 68(1):109–120. [https://doi.org/10.1016/S0038-092X\(99\)00047-X](https://doi.org/10.1016/S0038-092X(99)00047-X)
247. Fernández-Ibáñez P, Blanco J, Malato S, De Las Nieves FJ (2003) Application of the colloidal stability of TiO₂ particles for recovery and reuse in solar photocatalysis. *Water Res* 37(13):3180–3188. [https://doi.org/10.1016/S0043-1354\(03\)00157-X](https://doi.org/10.1016/S0043-1354(03)00157-X)
248. Makovec D, Sajko M, Selišnik A, Drogenik M (2011) Magnetically recoverable photocatalytic nanocomposite particles for water treatment. *Mater Chem Phys* 129(1–2):83–89. <https://doi.org/10.1016/j.matchemphys.2011.03.059>
249. Vidal A, Diaz AI, El Hraiki A, Romero M, Muguruza I, Senhaji F, González J (1999) Solar photocatalysis for detoxification and disinfection of contaminated water: pilot plant studies. *Catal Today* 54(2–3):283–290. [https://doi.org/10.1016/S0920-5861\(99\)00189-3](https://doi.org/10.1016/S0920-5861(99)00189-3)
250. Hernández-Alonso MD, Tejedor-Tejedor I, Coronado JM, Anderson MA (2011) Operando FTIR study of the photocatalytic oxidation of methylcyclohexane and toluene in air over TiO₂-ZrO₂ thin films: Influence of the aromaticity of the target molecule on deactivation. *Appl Catal B* 101(3–4):283–293. <https://doi.org/10.1016/j.apcatb.2010.09.029>
251. Augugliaro V, Coluccia S, Loddo V, Marchese L, Martra G, Palmisano L, Schiavello M (1999) Photocatalytic oxidation of gaseous toluene on anatase TiO₂ catalyst: mechanistic aspects and FT-IR investigation. *Appl Catal B* 20(1):15–27. [https://doi.org/10.1016/S0926-3373\(98\)00088-5](https://doi.org/10.1016/S0926-3373(98)00088-5)
252. Fujishima A, Zhang X, Tryk DA (2008) TiO₂ photocatalysis and related surface phenomena. *Surf Sci Rep* 63(12):515–582. <https://doi.org/10.1016/j.surfrep.2008.10.001>
253. Hensch G, Deubener J (2012) Compatibility of antireflective coatings on glass for solar applications with photocatalytic properties. *Sol Energy* 86(3):831–836. <https://doi.org/10.1016/j.solener.2011.12.010>
254. Demirbas A (2008) Biofuels sources, biofuel policy, biofuel economy and global biofuel projections. *Energy Convers Manage* 49(8):2106–2116. <https://doi.org/10.1016/j.enconman.2008.02.020>
255. Demirbas A (2011) Competitive liquid biofuels from biomass. *Appl Energy* 88(1):17–28. <https://doi.org/10.1016/j.apenergy.2010.07.016>
256. Gupta PK, Khan ZH, Solanki PR (2018) Effect of nitrogen doping on structural and electrochemical properties of zirconia nanoparticles. *Adv Sci Lett* 24(2):867–872. <https://doi.org/10.1166/asl.2018.10863>
257. Clavero C (2014) Plasmon-induced hot-electron generation at nanoparticle/metal-oxide interfaces for photovoltaic and photocatalytic devices. *Nat Photonics* 8(2):95–103. <https://doi.org/10.1038/nphoton.2013.238>
258. Iavicoli I, Leso V, Ricciardi W, Hodson LL, Hoover MD (2014) Opportunities and challenges of nanotechnology in the green economy. *Environ Health* 13(1):1–11. <https://doi.org/10.1186/1476-069X-13-78>
259. Lalitha G, Hemamalini R, Mu N (2018) Efficient photocatalytic degradation of toxic dyes using nanostructured TiO₂/polyaniline nanocomposite. *Desalin Water Treat* 108:322–328. <https://doi.org/10.5004/dwt.2018.21967>
260. McGuigan KG, Conroy RM, Mosler HJ, du Preez M, Ubomba-Jaswa E, Fernandez-Ibanez P (2012) Solar water disinfection (SODIS): a review from bench-top to roof-top. *J Hazard Mater* 235:29–46. <https://doi.org/10.1016/j.jhazmat.2012.07.053>
261. Clasen T, McLaughlin C, Nayaar N, Boisson S, Gupta R, Desai D, Shah N (2008) Microbiological effectiveness and cost of disinfecting water by boiling in semi-urban India. *Am J Trop Med Hyg* 79(3):407–413. <https://doi.org/10.4269/ajtmh.2008.79.407>
262. Kumar A, Naushad M, Rana A, Sharma G, Ghfar AA, Stadler FJ, Khan MR (2017) ZnSe-WO₃ nano-hetero-assembly stacked on Gum ghatti for photo-degradative removal of Bisphenol A: Symbiotic of adsorption and photocatalysis. *Int J Biol Macromol* 104:1172–1184. <https://doi.org/10.1016/j.ijbiomac.2017.06.116>
263. Alrousan DMA, Polo-López MI, Dunlop PSM, Fernández-Ibáñez P, Byrne JA (2012) Solar photocatalytic disinfection of water with immobilised titanium dioxide in re-circulating flow CPC reactors. *Appl Catal B* 128:126–134. <https://doi.org/10.1016/j.apcatb.2012.07.038>
264. Islam SZ, Nagpure S, Kim DY, Rankin SE (2017) Synthesis and catalytic applications of non-metal doped mesoporous titania. *Inorganics* 5(1):15. <https://doi.org/10.3390/inorganics5010015>
265. Goodarzi N, Ashrafi-Peyman Z, Khani E, Moshfeqh AZ (2023) Recent progress on semiconductor heterogeneous photocatalysts in clean energy production and environmental remediation. *Catalysts* 13(7):1102

266. Gulati S, Vijayan S, Kumar S, Harikumar B, Trivedi M, Varma RS (2023) Recent advances in the application of metal-organic frameworks (MOFs)-based nanocatalysts for direct conversion of carbon dioxide (CO₂) to value-added chemicals. *Coord Chem Rev* 474:214853
267. Rafiq A, Ikram M, Ali S, Niaz F, Khan M, Khan Q, Maqbool M (2021) Photocatalytic degradation of dyes using semiconductor photocatalysts to clean industrial water pollution. *J Ind Eng Chem* 97:111–128
268. Solayman HM, Hossen MA, Abd Aziz A, Yahya NY, Hon LK, Ching SL, Monir MU, Zoh KD (2023) Performance evaluation of dye wastewater treatment technologies: a review. *J Environ Chem Eng* 11:109610
269. Zhang L-L, Zaoui A, Sekkal W, Zheng Y-Y (2023) Interlayer adsorption of cationic dye on cationic surfactant-modified and unmodified montmorillonite. *J Hazard Mater* 442:130107
270. Lin Z, Wang R, Tan S, Zhang K, Yin Q, Zhao Z, Gao P (2023) Nitrogen-doped hydrochar prepared by biomass and nitrogen-containing wastewater for dye adsorption: effect of nitrogen source in wastewater on the adsorption performance of hydrochar. *J Environ Manag* 334:117503
271. Chiu Y-H, Chang T-FM, Chen C-Y, Sone M, Hsu Y-J (2019) Mechanistic insights into photodegradation of organic dyes using heterostructure photocatalysts. *Catalysts* 9:430
272. Silori R, Shrivastava V, Singh A, Sharma P, Aouad M, Mählknecht J, Kumar M (2022) Global groundwater vulnerability for pharmaceutical and personal care products (PPCPs): the scenario of second decade of 21st century. *J Environ Manag* 320:115703
273. Kumar M, Sridharan S, Sawarkar AD, Shakeel A, Anerao P, Mannina G, Sharma P, Pandey A (2023) Current research trends on emerging contaminants pharmaceutical and personal care products (PPCPs): a comprehensive review. *Sci Total Environ* 859:160031
274. Zhang C, Chen Y, Chen S, Guan X, Zhong Y, Yang Q (2023) Occurrence, risk assessment, and in vitro and in vivo toxicity of antibiotics in surface water in China. *Ecotoxicol Environ Saf* 255:114817
275. Chen X, Lei L, Liu S, Han J, Li R, Men J, Li L, Wei L, Sheng Y, Yang L (2021) Occurrence and risk assessment of pharmaceuticals and personal care products (PPCPs) against COVID-19 in lakes and WWTP-river-estuary system in Wuhan. *China Sci Total Environ* 792:148352
276. Rapti I, Boti V, Albanis T, Konstantinou I (2023) Photocatalytic degradation of psychiatric pharmaceuticals in hospital WWTP secondary effluents using G-C₃N₄ and g-C₃N₄/MoS₂ catalysts in laboratory-scale pilot. *Catalysts* 13:252
277. Kim J, Choi W (2010) Hydrogen producing water treatment through solar photocatalysis. *Energy Environ Sci* 3:1042–1045
278. Nugmanova AG, Safonova EA, Baranchikov AE, Tameev AR, Shkolin AV, Mitrofanov AA, Eli-seev AA, Meshkov IN, Kalinina MA (2022) Interfacial self-assembly of porphyrin-based SUR-MOF/graphene oxide hybrids with tunable pore size: an approach toward size-selective ambivalent heterogeneous photocatalysts. *Appl Surf Sci* 579:152080
279. Nikoloudakis E, Alsaleh AZ, Charalambidis G, Coutsolelos AG, D'Souza F (2022) A covalently linked nickel (II) porphyrin–ruthenium (II) tris (bipyridyl) dyad for efficient photocatalytic water oxidation. *Chem Commun* 58:12078–12081
280. Masood H, Toe CY, Teoh WY, Sethu V, Amal R (2019) Machine learning for accelerated discovery of solar photocatalysts. *Acs Catal* 9:11774–11787
281. Oral B, Can E, Yildirim R (2022) Analysis of photoelectrochemical water splitting using machine learning. *Int J Hydrog Energy* 47:19633–19654
282. Wang Z, Gu Y, Zheng L, Hou J, Zheng H, Sun S, Wang L (2022) Machine learning guided dopant selection for metal oxide-based photoelectrochemical water splitting: the case study of Fe₂O₃ and CuO. *Adv Mater* 34:2106776

Authors and Affiliations

Mohamed A. Hassaan¹ · Mohamed A. El-Nemr² · Marwa R. Elkatory³ · Safaa Ragab¹ · Violeta-Carolina Niculescu⁴ · Ahmed El Nemr¹ 

✉ Mohamed A. Hassaan
mhss95@mail.com

✉ Ahmed El Nemr
ahmedmoustafaelnemr@yahoo.com; ahmed.m.elnemr@gmail.com

Mohamed A. El-Nemr
mohamedelnemr1992@yahoo.com

Marwa R. Elkatory
marwa_elkatory@yahoo.com

Safaa Ragab
safaa_ragab65@yahoo.com

Violeta-Carolina Niculescu
violeta.niculescu@icsi.ro

¹ Marine Pollution Department, Environment Division, National Institute of Oceanography and Fisheries (NIOF), Kayet Bey, Elanfoushy 21556, Alexandria, Egypt

² Department of Chemical Engineering, Faculty of Engineering, Minia University, Minia 61519, Egypt

³ Advanced Technology and New Materials Research Institute, SRTA-City, New Borg El-Arab City 21934, Alexandria, Egypt

⁴ National Research and Development Institute for Cryogenic and Isotopic Technologies-ICSI Rm. Valcea, 4th Uzinei Street, 240050 Valcea, Romania